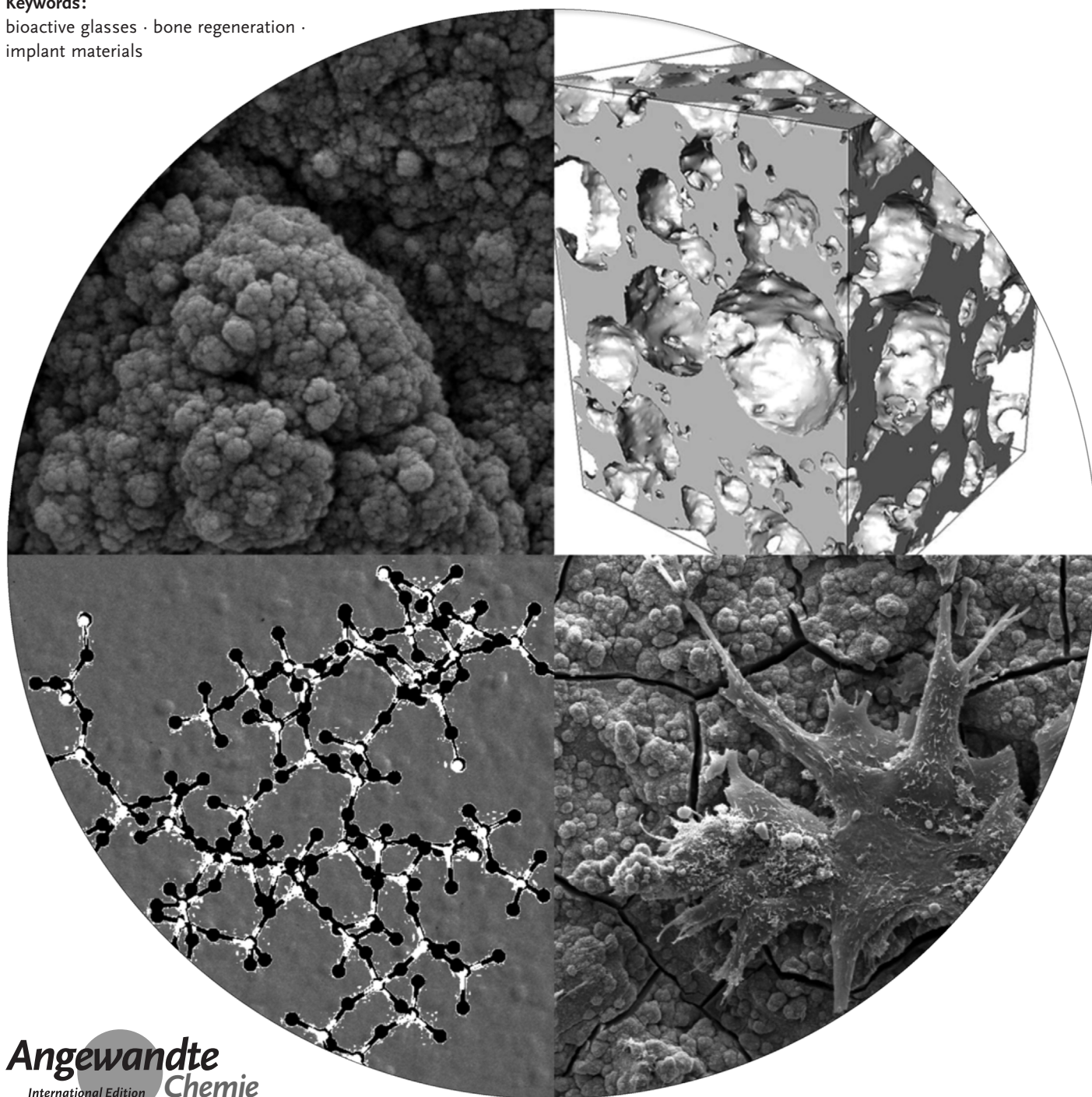


# Bioactive Glasses—Structure and Properties

Delia S. Brauer\*

**Keywords:**

bioactive glasses · bone regeneration ·  
implant materials



**B**ioactive glasses were the first synthetic materials to show bonding to bone, and they are successfully used for bone regeneration. They can degrade in the body at a rate matching that of bone formation, and through a combination of apatite crystallization on their surface and ion release they stimulate bone cell proliferation, which results in the formation of new bone. Despite their excellent properties and although they have been in clinical use for nearly thirty years, their current range of clinical applications is still small. Latest research focuses on developing new compositions to address clinical needs, including glasses for treating osteoporosis, with antibacterial properties, or for the sintering of scaffolds with improved mechanical stability. This Review discusses how the glass structure controls the properties, and shows how a structure-based design may pave the way towards new bioactive glass implants for bone regeneration.

## 1. Introduction

Humans have been using glass for thousands of years, from the first uses of natural glass (e.g. obsidian, a volcanic glass) for tools and arrow heads, to the early man-made glass beads and drinking vessels in Mesopotamia and Egypt.<sup>[1]</sup> In later times, glass became widely used for decorative articles, optics, architectural purposes (from windows to whole glass facades), glassware for chemical reactions, and fibers for telecommunication applications. Bioactive glasses, by contrast, are a relatively young group of materials.

The first biomaterials and implant materials were chosen to be as inert as possible, to avoid any foreign body reactions.<sup>[2]</sup> More recently, bioactive materials which “*elicit a specific biological response at the interface of the material which results in the formation of a bond between the tissues and the material*”<sup>[3]</sup> have been favored, among them bioactive glasses. Instead of being inert, bioactive glasses actually interact with the body tissue, thereby resulting in the formation of a strong interfacial bond between the implant (bioactive glass) and the bone. Additionally, they degrade over time,<sup>[4]</sup> allowing for the controlled release of therapeutically active ions and enabling bone regeneration rather than replacement, thereby restoring the original bone state and function.

In 1969, the first bioactive glass (Bioglass 45S5) was developed by L. Hench,<sup>[5]</sup> and it has been in clinical use since 1985. 45S5 has a composition of 46.1 SiO<sub>2</sub>, 2.6 P<sub>2</sub>O<sub>5</sub>, 24.4 Na<sub>2</sub>O, 26.9 CaO (in mol%), and many bioactive glasses consist of the same components, in slightly different concentrations (some representative bioactive glass compositions are shown in Table 1). However, how do bioactive glasses differ from the glasses we normally deal with? How can a glass, a material generally considered to be rather inert, be used not only to replace human bone, but also to regenerate it? And what causes it to not only allow for new bone formation but to actively stimulate and enhance it? These are, among others, the questions this Review aims to address. Current knowledge and understanding of how bioactive glass

## From the Contents

1. Introduction	4161
2. Glass Structure	4161
3. What Makes Glasses Bioactive?	4167
4. Crystallization and Processing	4171
5. Bioactivity of Glasses	4174
6. Summary and Outlook	4177

composition and particularly structure define their properties will be considered, and how this knowledge can be used to design bioactive glasses to give the required properties will be discussed.

Some of the questions addressed here are still under debate and will need several more years of research to be fully understood, but nonetheless looking into them will further our understanding of these glasses. Most importantly, however, this Review aims at creating interest in this fascinating class of materials.

## 2. Glass Structure

While glass has been used for a long time, the science of glass structure is relatively young, with the earliest publications dating from the 1920s.<sup>[6]</sup> New glass compositions used to be developed by a trial and error approach combined with the knowledge accumulated by glass technologists through years of experience. An increased understanding of how glass properties vary with composition and structure helps glass scientists to control glass properties, tailoring them to specific requirements, which improves understanding and facilitates interpretation of experimental results.

Glasses have two things in common: their amorphous structure and their temperature behavior, which shows a glass transition range ( $T_g$ ), which is the temperature interval where a system transforms from a supercooled liquid to a solid glass. In contrast to crystalline solids (Figure 1 a), glasses have no long-range order (Figure 1 b–d). In addition, when heating glasses, they show a smooth decrease in their viscosity by several orders of magnitude, which is the reason why glasses can be processed easily into various shapes.<sup>[12]</sup>

Oxide glasses are conventionally produced by melting the precursors (inorganic oxides, carbonates, fluorides, and

[\*] Jun.-Prof. Dr. D. S. Brauer  
Otto Schott Institute of Materials Research  
Friedrich Schiller University Jena  
Fraunhoferstrasse 6, 07743 Jena (Germany)  
E-mail: delia.brauer@uni-jena.de  
Homepage: <http://www.brauergroup.uni-jena.de>

**Table 1:** Selected bioactive glass compositions (mol%) and network connectivity (Section 2.1) of the silicate network ( $NC_{Si}$ ).

	SiO <sub>2</sub>	P <sub>2</sub> O <sub>5</sub>	Na <sub>2</sub> O	CaO	CaF <sub>2</sub>	K <sub>2</sub> O	MgO	$NC_{Si}$
45S5 <sup>[3a]</sup>	46.1	2.6	24.4	26.9	—	—	—	2.11
45S5F <sup>[7]</sup>	46.1	2.6	24.4	13.45	13.45	—	—	2.70
S53P4 <sup>[8]</sup>	53.9	1.7	22.7	21.8	—	—	—	2.54
13-93 <sup>[9]</sup>	54.6	1.7	6	22.1	—	7.9	7.7	2.59 <sup>[a]</sup>
6P61 <sup>[10]</sup>	61.0	2.5	10.0	13.5	—	2.4	10.7	3.05 <sup>[a]</sup>
6P55 <sup>[10]</sup>	54.1	2.5	11.5	15.9	—	3.4	12.6	2.67 <sup>[a]</sup>
6P50 <sup>[10]</sup>	49.4	2.5	14.9	16.6	—	3.5	13.2	2.36 <sup>[a]</sup>
ICIE1 <sup>[11]</sup>	49.46	1.07	26.38	23.08	—	—	—	2.11
ICIE16 <sup>[11]</sup>	49.46	1.07	6.6	36.27	—	6.6	—	2.11

[a] Calculated assuming MgO acts as a modifier (see Section 2.2).

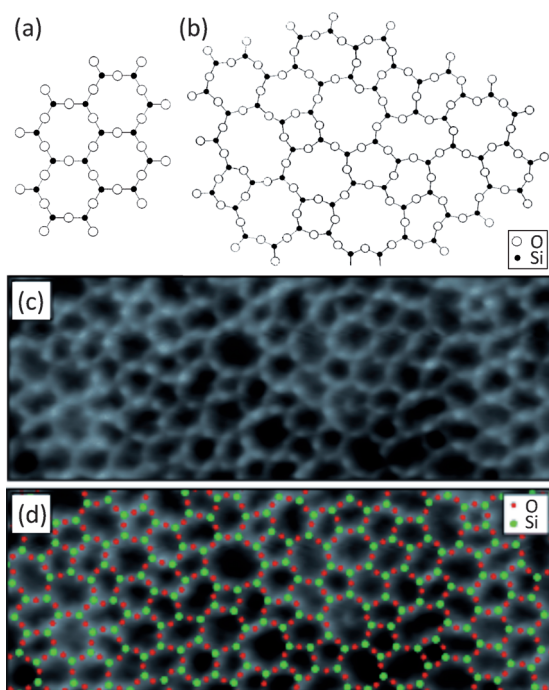


**Figure 1.** Structure of a) crystalline and b) vitreous silica (only three oxygen atoms are shown per SiO<sub>4</sub> tetrahedron, with the fourth lying above or below the image plane),<sup>[13]</sup> c) atomic-resolution scanning tunneling microscopy image of a vitreous SiO<sub>2</sub> film, and d) the same image superimposed with a schematic representation of oxygen and silicon atoms.<sup>[14]</sup>



Delia S. Brauer was born in Berlin, Germany. After finishing her studies in environmental chemistry she completed her PhD (under the supervision of Prof. Christian Rüssel) on phosphate glasses at the University of Jena. After postdoctoral research at the University of California, San Francisco, USA, Nagoya Institute of Technology, Japan, as well as Imperial College London and Queen Mary, University of London, UK, in 2012 she returned to Jena as a junior professor at the Otto Schott Institute of Materials Research. Her research focuses on degradable and highly disrupted glass systems including bioactive glasses. She is a member of Technical Committee 04 (Bioglasses) of the International Commission on Glass and Associate Editor of a new journal "Biomedical Glasses".

others) in precious metal or ceramic crucibles at high temperatures, which is typically between 1200 and 1500 °C for bioactive glasses but depends on the composition. If the cooling is rapid enough, crystallization will be inhibited and a glass will result. Another common way of preparing bioactive glasses is by a polycondensation reaction from organic precursors (alkoxides such as tetraethyl orthosilicate),<sup>[15]</sup> but these sol-gel-derived glasses are beyond the scope of this Review.

### 2.1. Silicate Structure of Bioactive and Conventional Glasses

Three different components are usually described within the glass structure. *Network formers* are able to form glasses without the need for additional components, and they include silica (SiO<sub>2</sub>), phosphorus pentoxide (P<sub>2</sub>O<sub>5</sub>), and boron trioxide (B<sub>2</sub>O<sub>3</sub>). The basic building unit of silicate glasses is the SiO<sub>4</sub> tetrahedron, which can be connected to neighboring SiO<sub>4</sub> tetrahedra through Si-O-Si bonds, commonly referred to as bridging oxygen atoms. These tetrahedra are commonly referred to as  $Q^n$  units, where  $n$  describes the number of bridging oxygen atoms connected to the tetrahedron. In vitreous silica, each tetrahedron is linked to another one at each of its four corners, which corresponds to four bridging oxygen atoms per tetrahedron ( $Q^4$  units).

*Network modifiers*, by contrast, alter the glass structure by turning bridging oxygen atoms (with chemical bonds predominantly covalent in character) into nonbridging oxygen atoms (Si-O<sup>-</sup>M<sup>+</sup> linkages, predominantly ionic in character, where M<sup>+</sup> is a modifier cation).<sup>[12]</sup> Typical modifiers include the oxides of alkali or alkaline-earth metals, and unlike network former cations, which are typically three- or fourfold coordinated, modifier cations show higher coordination numbers according to neutron diffraction and molecular dynamics (MD) simulation experiments. Typical examples are sodium (coordination number: 5.6 to 6), calcium (6–6.3), and strontium (6.7–7.1).<sup>[16]</sup>

The third category of components are the *intermediate oxides*, which can act like typical network modifiers<sup>[17]</sup> or may possibly enter the backbone of the glass structure<sup>[18]</sup> (acting more like a network former), and which will be discussed in Section 2.4.

<sup>29</sup>Si magic-angle-spinning (MAS) NMR spectroscopy has been used successfully to characterize the silicate structure of



bioactive glasses,<sup>[11,20]</sup> as different  $Q$  species have different chemical shifts. Owing to broad signals, however, deconvolution of the spectra is generally necessary, which tends to be somewhat arbitrary, and indeed both binary models<sup>[20,21]</sup> (assuming the presence of  $Q^2$  and  $Q^3$  units only in bioactive glasses) and ternary models<sup>[19]</sup> ( $Q^1$ ,  $Q^2$ , and  $Q^3$ ) have been used. Either way, the signal maximum lies at about  $-80$  ppm (Figure 2), which corresponds to a structure consisting of

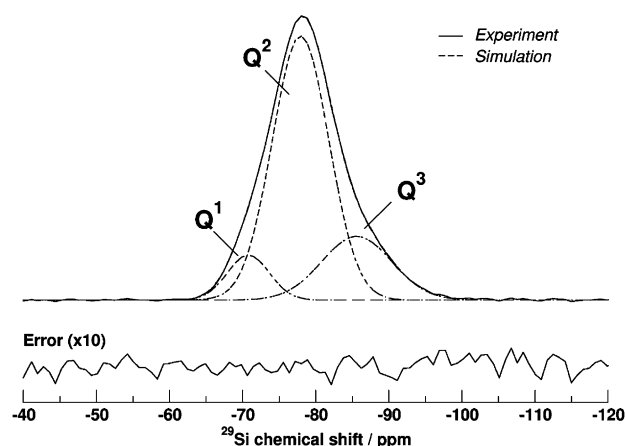


**Figure 2.** Experimental  $^{29}\text{Si}$  MAS NMR spectrum and fit (to obtain individual signals for  $Q^1$ ,  $Q^2$ , and  $Q^3$  units) by MD simulation.<sup>[19]</sup>

mainly  $Q^2$  groups and shows that their structure is very disrupted compared to conventional glasses, which commonly consist mostly of  $Q^3$  and  $Q^4$  groups. MD simulations illustrate how increasing amounts of modifiers result in more non-bridging oxygen atoms being present (Figure 3).<sup>[22]</sup> The glass on the left-hand side of Figure 3 is the well-known Bioglass 45S5 (Table 1), while the other two glasses contain smaller amounts of calcium and sodium oxide (56.5  $\text{SiO}_2$ , 2.6  $\text{P}_2\text{O}_5$ , 19.4  $\text{Na}_2\text{O}$ , 21.5  $\text{CaO}$  and 66.9  $\text{SiO}_2$ , 2.6  $\text{P}_2\text{O}_5$ , 14.5  $\text{Na}_2\text{O}$ , 16.0  $\text{CaO}$ , respectively, all in mol %). MD simulations have also shown the more open, less cross-linked silicate network of bioactive glasses to consist of not only chains but also rings (Figure 4 a,b).<sup>[16b]</sup>

The glass structure can be estimated based on the glass composition, and the *network connectivity* ( $\text{NC}_{\text{Si}}$ )<sup>[23]</sup> model describes the average number of bridging oxygen atoms per

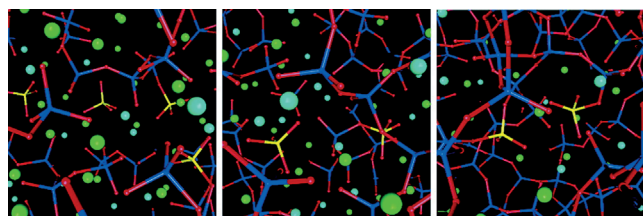


**Figure 3.** Structure of bioactive glasses with 46.1 mol % (Bioglass 45S5, left), 56.5 mol % (BG55, center), and 66.9 mol %  $\text{SiO}_2$  (BG65, right) obtained from classical MD simulation, showing a decreasing number of modifier cations (spheres) and a more-cross-linked network from left to right. (O red, Si blue, P yellow, Na dark green, Ca cyan; sodium and calcium ions are shown as spheres, whereas silicon, phosphorus, and oxygen are shown as ball and stick models.)<sup>[22]</sup>

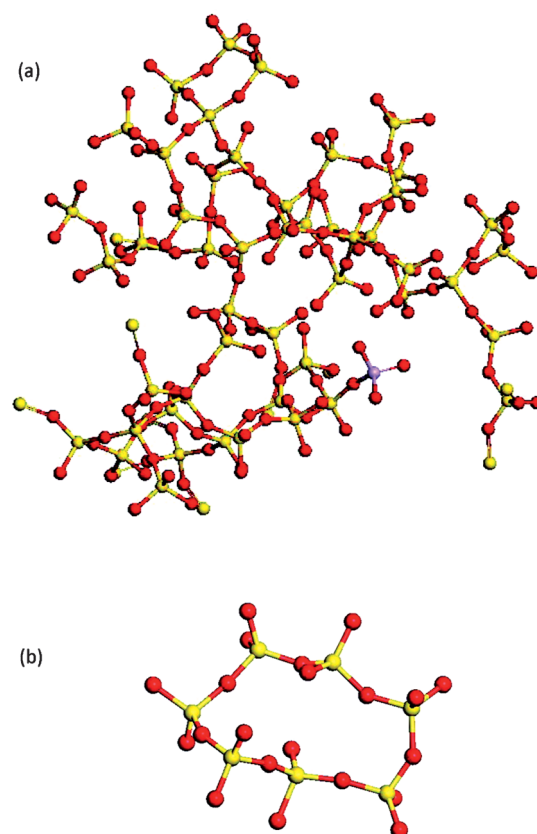


**Figure 4.** Structure of Bioglass 45S5 obtained using MD simulation: a) the silicate ( $\text{SiO}_4$ ) backbone and b) a seven-membered silicate ring representing short silicate units (O red, Si yellow, P purple).<sup>[16b]</sup>

network-forming element (here: silicon,  $\text{NC}_{\text{Si}}$ ). The network connectivity gives an idea of the average polymerization of the network,<sup>[24]</sup> while it is also a useful tool<sup>[23b]</sup> for predicting glass properties such as bioactivity, crystallization tendency, and glass transition temperature.<sup>[25]</sup>

The network connectivity of simple  $\text{SiO}_2$ - $\text{P}_2\text{O}_5$ - $\text{M}_2\text{O}$ - $\text{M}'\text{O}$  bioactive glasses (where  $\text{M}_2\text{O}$  and  $\text{M}'\text{O}$  are network modifiers) is calculated according to Equation (1), which assumes a maximum of four bridging oxygen atoms per silicon atom, of which the nonbridging oxygen atoms formed by modifiers are subtracted.  $\text{P}_2\text{O}_5$  increases the number of bridging oxygen atoms as it needs modifier cations to balance the charge of  $\text{PO}_4^{3-}$  (see Section 2.2).<sup>[23]</sup>  $\text{SiO}_2$ ,  $\text{P}_2\text{O}_5$ ,  $\text{M}_2\text{O}$ , and  $\text{M}'\text{O}$  refer to the molar percentages of each component.

$$\text{NC}_{\text{Si}} = \frac{4 \times \text{SiO}_2 + 6 \times \text{P}_2\text{O}_5 - 2 \times (\text{M}_2\text{O} + \text{M}'\text{O})}{\text{SiO}_2} \quad (1)$$

Vitreous silica has a network connectivity of four, and the network connectivity decreases as the network modifier content increases. Bioactive glasses usually have network connectivities between 2 and 3 (Table 1), with Bioglass 45S5 having a network connectivity of 2.11, which corresponds to a structure consisting of silicate chains (89%  $Q^2$ ), in which 11% of all  $Q$  units are branching units ( $Q^3$ ) that interconnect the chains by bridging oxygen atoms.



By contrast, the *network rigidity* model (also referred to as the “floppy networks” model)<sup>[26]</sup> takes into account local variation of the structure, described as “rigid” and “floppy” regions. This approach is particularly interesting for more-cross-linked glasses, for example, bioactive glasses with a network connectivity above 2.4. Based on the concepts published by Phillips and Thorpe<sup>[27]</sup> the network rigidity model describes how, for three-dimensional networks (such as silicate glass networks), the network becomes rigid above the percolation point, which corresponds to a network connectivity of 2.4. Below this point, the network can be described as floppy. However, even in rigid networks, floppy regions exist, the size of which can be estimated based on the glass composition.<sup>[26]</sup> As will be seen later, these floppy regions help to understand and explain the properties of bioactive glasses of higher network connectivity.

## 2.2. Phosphate Structure of Bioactive Glasses

Many bioactive glasses contain a second network former,  $P_2O_5$ , besides  $SiO_2$ . It has been assumed for a long time that this results in a mixed silicate/phosphate network containing Si-O-P bonds,<sup>[23a]</sup> a view which has been supported by results from molecular dynamics simulations.<sup>[22]</sup> Based on  $^{31}P$  MAS NMR experiments, however, it has been shown that bioactive glasses contain phosphate as orthophosphate ( $PO_4^{3-}$ ), no matter if the glasses are annealed<sup>[20]</sup> or quenched only.<sup>[11]</sup> A recent study combining first-principles simulations with  $^{17}O$  and 3QMAS (triple quantum MAS) NMR spectroscopy on  $^{17}O$ -enriched 45S5 and  $^{31}P$  MAS NMR spectroscopy on 45S5 confirmed the absence of Si-O-P bonds in bioactive glasses,<sup>[19]</sup> while another recent study showed that while the majority of phosphorus atoms are present as orthophosphate, small amounts of Si-O-P bonds (8%) are also present.<sup>[28]</sup> Similarly, small amounts of pyrophosphate ( $P_2O_7^{4-}$ ) may<sup>[20,29]</sup> or may not<sup>[28]</sup> be present in some bioactive phosphosilicate glass compositions. Despite these discrepancies, all the  $^{31}P$  MAS NMR studies agree that phosphorus atoms are present mainly as orthophosphate in bioactive phosphosilicate glasses (Figure 5).

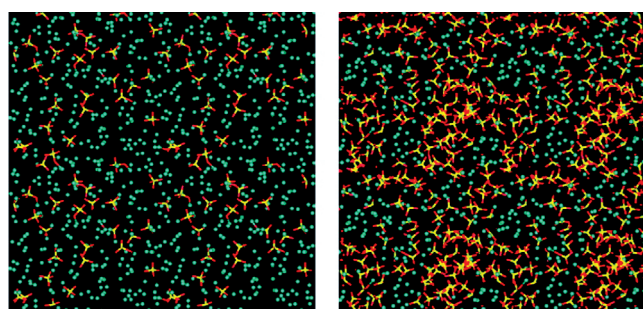


**Figure 5.** Phosphate environment in bioactive glasses obtained from MD simulation: individual (in 45S5, left) and clustered orthophosphate groups (in a glass with 12 mol%  $P_2O_5$ , right). Only the phosphate groups are displayed with silicon atoms represented as spheres (Si turquoise, P yellow, O red), and modifier cations omitted.<sup>[30]</sup>

These orthophosphate groups are surrounded by modifier cations for charge-balancing purposes. While MD simulation experiments<sup>[30]</sup> have reported a preference of orthophosphate for sodium ions at low  $P_2O_5$  contents in bioactive  $SiO_2$ - $P_2O_5$ - $Na_2O$ - $CaO$  glasses and for calcium at high  $P_2O_5$  contents,  $^{31}P$  MAS NMR experiments by a number of researchers<sup>[11,20,21,29a]</sup> investigating similar glass systems (containing sodium and calcium ions as modifiers only) suggest that  $Ca^{2+}$  and  $Na^+$  partition randomly between the silicate part of the glass structure and the phosphate part.  $^{31}P$  MAS NMR data give a continuous change in the isotropic chemical shift from that of sodium orthophosphate (14 ppm) to that of calcium orthophosphate (3 ppm), with the  $CaO/(CaO + Na_2O)$  ratio changing from 0 to 1 (Figure 6). This means that the Ca/Na ratio of cations charge-balancing the  $Q_P^0$  and  $Q_{Si}^n$  units is the same, each representing the overall Ca/Na ratio in the glass. The reason may be that  $Ca^{2+}$  and  $Na^+$  have comparable ionic radii,<sup>[31]</sup> as a preferential charge-balancing of orthophosphate by calcium rather than alkali metal cations has been detected

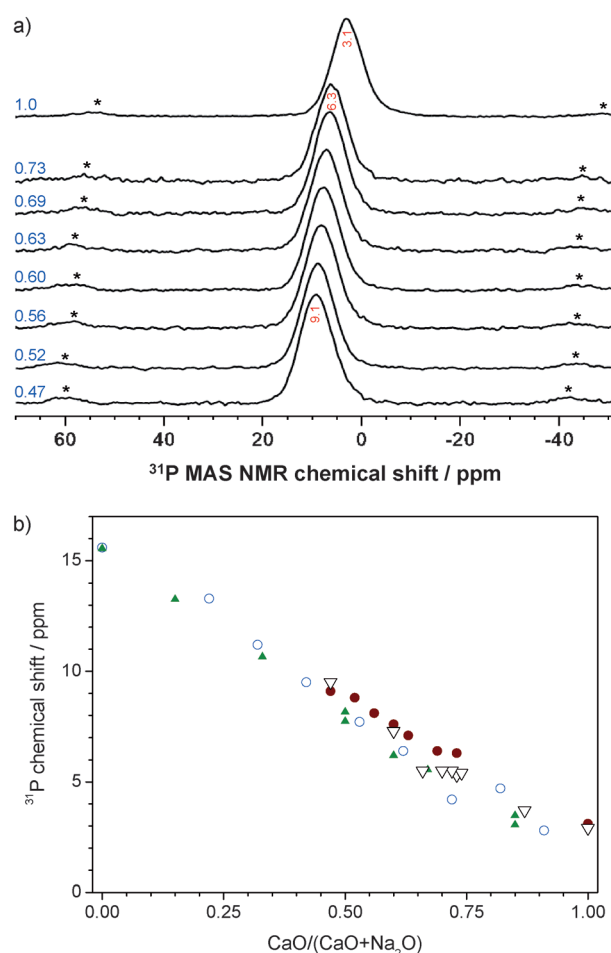


**Figure 6.** a)  $^{31}P$  MAS NMR spectra of bioactive glasses with different CaO to  $(CaO + Na_2O)$  ratios (in blue; chemical shift given in red)<sup>[21]</sup> b)  $^{31}P$  MAS NMR chemical shift versus  $CaO/(CaO + Na_2O)$  ratio in bioactive sodium calcium phosphosilicate glasses showing random partitioning of sodium and calcium ions between the phosphate and silicate phase (plotted using data presented by Elgayar et al. (open triangles),<sup>[11]</sup> Lockyer et al. (blue circles),<sup>[20]</sup> Grussaute et al. (green triangles),<sup>[29a]</sup> and Brauer et al. (red dots)<sup>[21]</sup>)

in calcium-, sodium-, and lithium-containing 45S5,<sup>[32]</sup> possibly caused by  $\text{Li}^+$  having a much smaller ionic radius than the other two ions.<sup>[31]</sup> Similarly, the presence of aluminum and gallium ions in the same glass also affected the sodium/calcium partitioning, thereby resulting in preferential charge-balancing of the orthophosphate by calcium rather than sodium ions.<sup>[33]</sup>

If phosphorus is present as orthophosphate (charge-balanced by modifier cations) in bioactive phosphosilicate glasses, this raises the question of whether those orthophosphate groups are present as individual, isolated tetrahedra within the silicate network (Figure 5, left), if the phosphate tetrahedra form clusters within the silicate network (as suggested by MD simulations on glasses with a high phosphate content, Figure 5, right), or if bioactive phosphosilicate glasses are *phase-separated* into a phosphate-rich droplet phase dispersed within a silicate-rich matrix.

Dielectric measurements on bioactive glasses (e.g. ICIE1, Table 1) showed two separate sodium-hopping processes,<sup>[34]</sup> which has been interpreted as indicating the presence of two separate phases.<sup>[35]</sup> In addition, high phosphate content bioactive glasses, when heat-treated, crystallize to orthophosphate species (including apatite),<sup>[36]</sup> while low phosphate content bioactive glasses showed either crystallization of silicate species<sup>[37]</sup> or minor amounts of phosphate species only.<sup>[38]</sup> This may indicate that the phosphate-rich regions are too small and too diluted in low phosphate content glasses to play a significant role in nucleation and crystallization. However, the phosphate-rich regions increase in size and number as the phosphate content increases, thus allowing for nucleation and crystallization of orthophosphate species. Recent solid-state NMR studies showed the presence of nanometer-sized, five- to six-membered phosphate clusters in bioactive phosphosilicate glasses,<sup>[28]</sup> while transmission electron microscopy (TEM) replica images of freshly fractured bioactive glass surfaces showed droplet-shaped regions, possibly indicating the presence of phase separation (Figure 7). In addition, phase separation has been suggested to be a precursor to crystallization in bioactive glasses of low network connectivity (45S5),<sup>[39]</sup> but not in those of higher network connectivity (S53P4).<sup>[40]</sup> This hypothesis suggests that phase separation may be important for controlling or preventing crystallization, and it is likely to depend on various factors including composition (network connectivity, phosphate content, type of modifiers) and glass treatment (fast quenching versus annealing).

### 2.3. Other Structural Elements in Bioactive Glasses

In the past it was assumed that *fluorine* atoms replace oxygen atoms in silicate glasses, thereby forming Si–F bonds.<sup>[41]</sup> In bioactive glasses, however, fluoride complexes the modifier cations ( $\text{Ca}^{2+}$ ,  $\text{Na}^+$  etc.) exclusively, with no detectable amount of Si–F bonds, as confirmed by  $^{19}\text{F}$  MAS NMR spectroscopy and MD simulation.<sup>[21,42]</sup> The fluoride environment in bioactive glasses, while being amorphous, shows similarities to the structure of fluorite ( $\text{CaF}_2$ ),<sup>[21,42b]</sup> and this, together with fluoride clustering (as shown by MD

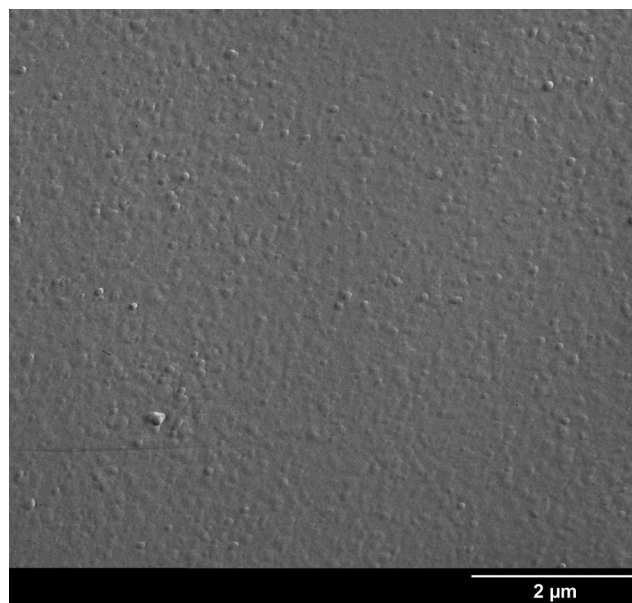


**Figure 7.** A TEM replica image of a freshly fractured bioactive glass (ICIE16, Table 1) surface showing droplet-shaped regions, possibly indicating phase separation.

simulations, Figure 8)<sup>[38]</sup> results in the crystallization of calcium fluoride at high fluoride concentrations in the glass.<sup>[37]</sup>

*Intermediate* ions have crystal field strengths lying in the range between those of network formers and modifiers,<sup>[41a,43]</sup> and as a result the incorporation of intermediate oxides into glasses can help to improve certain glass properties, such as reducing the tendency to crystallize. However, they tend to complicate the structure, as they can switch their role in the

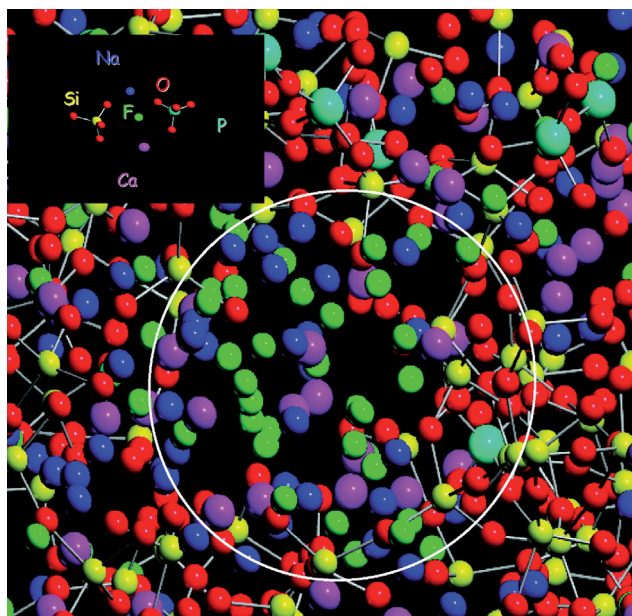


**Figure 8.** Fluoride environment in a bioactive glass (45S5 with 15% of  $\text{CaO}$  replaced by  $\text{CaF}_2$ ) obtained by MD simulation: the area in the white circle is enriched in fluoride ions (green), charge-balanced by calcium (pink) and sodium (blue) cations.<sup>[38]</sup>

glass. Magnesium<sup>[44]</sup> falls on the boundary between modifiers and intermediates according to Dietzel,<sup>[41a]</sup> and <sup>29</sup>Si MAS NMR experiments showed an increasingly polymerized silicate network with increasing MgO for CaO substitution in bioactive glass ICIE1.<sup>[18]</sup> The authors explained this by magnesium partially (about 15 %) switching its role to network former, entering the silicate network as MgO<sub>4</sub><sup>2-</sup> units. These MgO<sub>4</sub><sup>2-</sup> units would require modifier cations in their vicinity for charge-balancing purposes, thus effectively increasing the network connectivity of the silicate network, as these cations no longer create nonbridging oxygen atoms.<sup>[18]</sup> These findings agree with comparisons of the structure of SiO<sub>2</sub>-CaO and SiO<sub>2</sub>-MgO sol-gel glasses, where CaO was found to depolymerize the structure more than MgO.<sup>[45]</sup> Interestingly, MD simulations of conventional MgO-substituted soda lime silicate glasses (75 SiO<sub>2</sub>, 15 Na<sub>2</sub>O, (10-x) CaO, x MgO; x = 0–10 mol %)<sup>[46]</sup> showed about 90 % of the Mg<sup>2+</sup> participating in the silicate network as fourfold coordinated species (with the remaining ones being fivefold coordinated and acting as typical modifiers). However, comparable studies by the same authors<sup>[17]</sup> on MgO-substituted 45S5 (46.2 SiO<sub>2</sub>, 2.6 P<sub>2</sub>O<sub>5</sub>, 24.3 Na<sub>2</sub>O, (26.9-x) CaO, x MgO; x = 0–26.9 mol %) showed Mg<sup>2+</sup> to be present with fivefold coordination, thereby resulting in a constant network connectivity throughout the series. High-field <sup>25</sup>Mg MAS NMR results showed that the coordination number of magnesium ions in glassy and crystalline silicates is influenced not only by the network connectivity but also by the field strength of other modifier ions present, with the presence of higher field strength cations resulting in higher magnesium coordination numbers.<sup>[47]</sup>

Zinc, which also falls on the boundary between modifiers and intermediates,<sup>[41a]</sup> has also been suggested to partially enter the silicate network,<sup>[48]</sup> based on the detection of ZnO<sub>4</sub><sup>2-</sup> tetrahedra by Raman spectroscopy<sup>[49]</sup> and of Si-O-Zn bonds by deconvolution of <sup>29</sup>Si MAS NMR spectra<sup>[50]</sup> of zinc-containing bioactive glasses. In addition, neutron diffraction experiments showed cobalt and nickel ions in bioactive glasses to be present with both fivefold (67 % of Co or Ni) and fourfold (33 %) coordination, which the authors also interpreted as those elements partially entering the silicate network and acting as network formers.<sup>[51]</sup>

Substitution of different modifier cations has also been shown to affect the glass structure, despite the fact that the network connectivity remained constant. If sodium oxide is substituted for calcium oxide on a molar basis, it affects glass properties such as density, hardness, and crystallization temperature,<sup>[52]</sup> although the network connectivity and silicate network polymerization are maintained.<sup>[11]</sup> The reason is differences in the ionic radii and field strengths of the two ions, which also causes significantly higher glass transition (but also melting) temperatures of sodium-free compositions compared to sodium-containing ones.<sup>[21,36,37]</sup> When substituting modifier cations of the same valency but different sizes for each other (e.g. strontium for calcium<sup>[16b,53]</sup> or potassium for sodium),<sup>[32b]</sup> the silicate network has been shown to expand or become more compact,<sup>[32b,53a,54]</sup> depending on the size of the cations. This effect can be described by changes in the packing density of the glass, referred to as the oxygen packing density

or simply (if confusingly) oxygen density.<sup>[55]</sup> It has been shown to affect glass properties such as solubility and bioactivity.<sup>[56]</sup>

If sodium ions in glasses are gradually replaced by other alkali metal ions such as potassium or lithium, properties depending on transport mechanisms (including thermal properties and solubility) typically show nonlinear changes, an effect which is named the mixed alkali effect,<sup>[57]</sup> and which has also been observed in bioactive glasses<sup>[32b]</sup> and helps to reduce glass crystallization.<sup>[11]</sup>

## 2.4. The Importance of Glass Structure in Glass Design

Traditionally, the composition of bioactive glasses has been given in weight (rather than molar) percentages, but changing the glass composition based on weight percentages is not a good idea. This has been demonstrated by O'Donnell and Hill,<sup>[58]</sup> who showed that the differences in the atomic weights of calcium and strontium (40 and 88 g mol<sup>-1</sup>, respectively) resulted in substitutions by weight increasing the network connectivity dramatically and thus significantly reducing glass dissolution, ion release, and apatite formation. Generally, substituting one modifier for another on a molar basis will maintain the structure of the silicate network.

<sup>29</sup>Si MAS NMR experiments<sup>[59]</sup> showed that if P<sub>2</sub>O<sub>5</sub> is added to a bioactive glass without adding stoichiometric amounts of modifier oxides to allow for charge-balancing of PO<sub>4</sub><sup>3-</sup> groups, the orthophosphate groups will scavenge stoichiometric amounts of modifier cations from the silicate network, thereby changing the Q<sup>n</sup> speciation (Figure 9a), dramatically increasing the network connectivity of the silicate network,<sup>[29b,60]</sup> and decreasing the bioactivity at high phosphate content. By contrast, when adding P<sub>2</sub>O<sub>5</sub> together with stoichiometric amounts of network modifiers, the network connectivity remains constant (Figure 9b),<sup>[59]</sup> and the bioactivity increases with the phosphate content.<sup>[23b,61]</sup>

The substitution of intermediates for modifiers may affect the glass structure, for example, when substituting magnesium for calcium<sup>[18]</sup> or incorporating cobalt or nickel.<sup>[51]</sup> It is difficult to predict the exact changes in structure, as some intermediates tend to only partially enter the silicate network (if at all), and this makes structural analyses necessary. Such studies become even more important if additional network formers (such as B<sub>2</sub>O<sub>3</sub>) are incorporated into a glass, and ideally they should be substituted for network formers rather than modifiers.

MD simulations showed that if CaF<sub>2</sub> is substituted for modifier oxides (such as CaO), the fluoride anions remove modifier cations from the silicate network, thereby causing the silicate network to polymerize,<sup>[42a]</sup> increasing the network connectivity,<sup>[38,42c]</sup> and subsequently decreasing the bioactivity.<sup>[62]</sup> If CaF<sub>2</sub> is added to the glass by keeping the ratio of all other components constant, the network connectivity remains constant,<sup>[21]</sup> and changes in solubility and apatite formation are likely to be caused by calcium fluoride, rather than by changes in the silicate polymerization.<sup>[63]</sup>

Interpreting experimental data can be challenging at the best of times, but if several parameters are changed at once, such as the glass composition and structure of the silicate



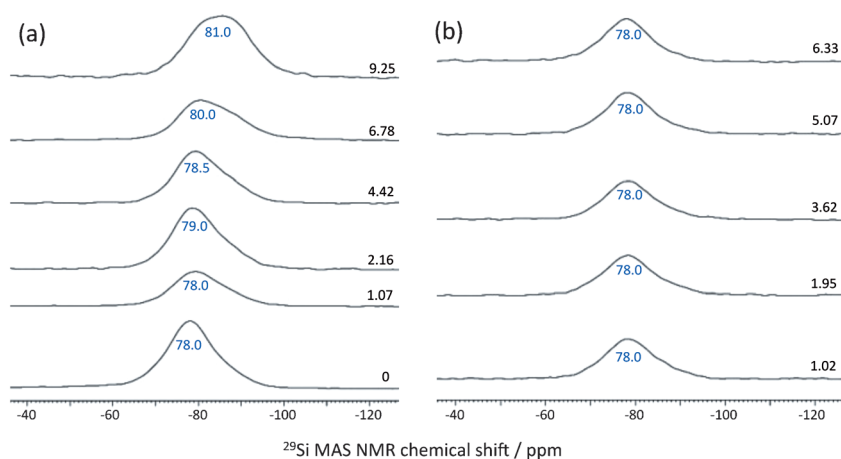


**Figure 9.** Changes in  $^{29}\text{Si}$  MAS NMR spectra when  $\text{P}_2\text{O}_5$  is added to a bioactive glass (51  $\text{SiO}_2$ , 26  $\text{Na}_2\text{O}$ , 23  $\text{CaO}$ , in mol %) a) without and b) with additional modifier cations for charge balancing: without additional modifiers, the silicate network is increasingly polymerized, moving from a  $\text{Q}^2$  to a  $\text{Q}^3$  structure, while with additional modifiers, the structure remains constant. Black numbers give  $\text{P}_2\text{O}_5$  content in mol %; blue numbers give the chemical shift of signal maximum. Modified from data by O'Donnell et al.<sup>[59]</sup> with permission from Elsevier.

network, it will be difficult, if not impossible, to correctly interpret the experimental findings and find the cause of an observed change in properties.

### 3. What Makes Glasses Bioactive?

It is the structural differences between conventional glasses and bioactive glasses with their more open silicate network (Figure 4) which cause the pronounced differences in their properties. When bioactive glasses are in contact with aqueous solutions (e.g. body fluids), they start to dissolve and release ions such as calcium and phosphate ions. One result of this ion release is the formation of an apatite surface layer, which is often, if incorrectly, referred to as “bioactivity”.<sup>[64]</sup> As the ability of bioactive glasses to react with water and degrade in the presence of aqueous solutions is key to their ability to release ions, form an apatite surface layer, and help to regenerate bone (and thus to their *in vivo* success), these processes will be reviewed in detail in the following sections.

#### 3.1. Solubility Behavior of Bioactive Glasses and the Influence of Glass Structure

The open silicate network of bioactive glasses allows water molecules to penetrate the glass network much more easily than in conventional glasses (Figure 10),<sup>[65]</sup> which results in significant differences between the dissolution patterns of bioactive and conventional glasses.<sup>[66]</sup> MD simulations

have illustrated this mechanism,<sup>[67]</sup> highlighting the importance of an open network for water intrusion, but also of surface features such as nonbridging oxygen atoms and modifier cations (Figure 10a). When silicate glasses come into contact with water, an ion exchange occurs at the glass/water interface between modifier ions, particularly  $\text{Na}^+$ , and protons from the solution.<sup>[68]</sup> MD simulations showed modifier cations acting as Lewis acids and, through interaction with water molecules, triggering  $\text{H}_2\text{O}$  dissociation and stabilizing the hydroxide ions.<sup>[69]</sup> The hydrophilic nonbridging oxygen atoms and modifier cations seem to be the active sites, which allow for strong interaction between the bioactive glass surface and water. By contrast, bridging oxygen atoms are more hydrophobic, and no significant interaction has been observed.<sup>[67]</sup>

In dynamic dissolution experiments,<sup>[66]</sup> conventional glasses showed a short burst of modifier ion release followed by negligible ion release during the remaining time of the experiment. This suggests that network modifiers were released near the glass surface only, with the bulk of the glass being unaffected. Bioactive glasses, by contrast, showed a pronounced release of ions throughout the experiment, thus suggesting the release of modifier ions from deeper within the bulk.<sup>[66]</sup> This ion exchange results in a fast and pronounced pH increase (Figure 11),<sup>[61,63]</sup> with most of the pH change occurring during the first few minutes to hours.<sup>[66]</sup>

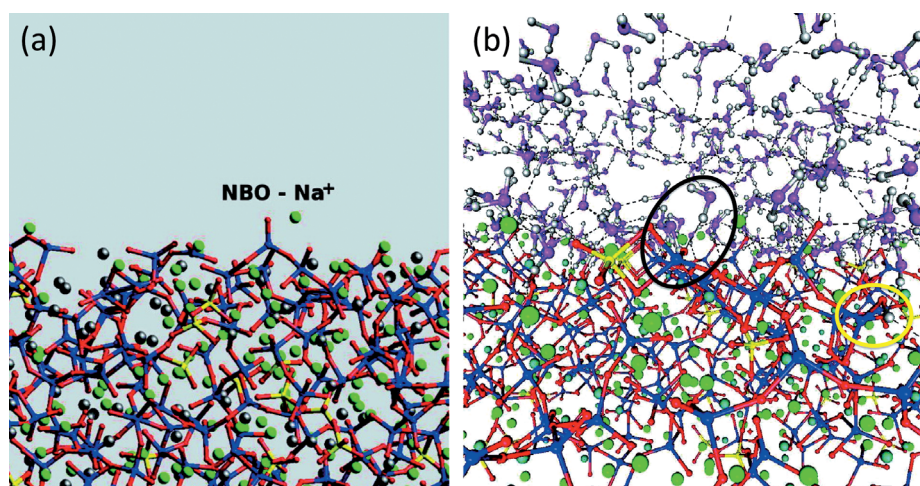


**Figure 10.** a) Bioactive glass features affecting bioactivity, including an open, disrupted silicate network and nonbridging oxygen atoms (NBOs) and modifier cations (here:  $\text{Na}^+$ ) near the glass surface (color codes O red, Si blue, Na green, Ca dark gray, P yellow), obtained from MD simulations.<sup>[65]</sup> b) Interaction at the bioactive glass/water interface (color codes  $\text{O}_{\text{glass}}$  red,  $\text{O}_{\text{water}}$  purple, H white, Si blue, Na green, Ca turquoise, P yellow; dashed lines: hydrogen bonds) showing hydrogen bonds between water molecules and  $\text{O}_{\text{glass}}$  (black circle) and Si-OH groups (yellow circle), obtained from Carr–Parrinello MD simulation.<sup>[67]</sup>

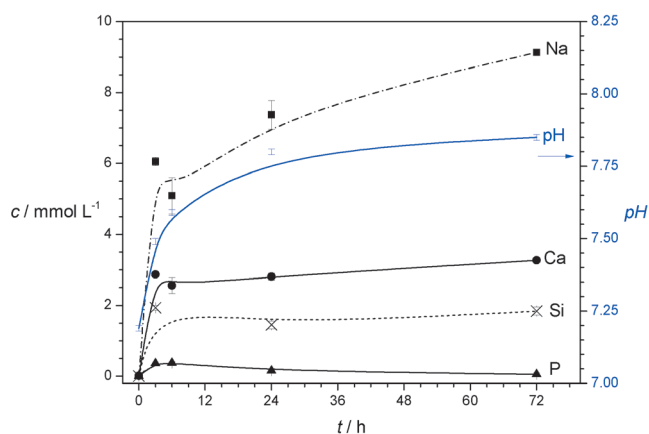


**Figure 11.** pH changes (blue, right axis) and released ions (black, left axis) upon immersion of 45S5 glass powder in Tris-HCl buffer solution.

In conventional silicate glasses, the leaching of modifier ions from the glass surface can result in the formation of a protective surface film, which is silica-rich compared to the bulk of the glass.<sup>[70]</sup> The formation of a modifier-depleted, silica-rich surface layer is also commonly observed on bioactive glasses,<sup>[63,70,71]</sup> however, because of their open silicate network allowing for deeper water penetration, this silica gel layer does not act as a protective film here, and ions (modifier and orthophosphate ions, as well as silicon-containing species, Figure 11) are continuously released from the glass.<sup>[66]</sup>

According to the original mechanism of bioactivity published by Hench,<sup>[72]</sup> the initial ion exchange and pH rise is followed by alkaline hydrolysis of Si-O-Si bonds and subsequent condensation reactions between Si-OH groups, which leads to repolymerization of a silica gel layer. According to studies on the corrosion of silicate glasses by Hench and co-authors,<sup>[68,70]</sup> a pH value of at least 9 to 10 is necessary to cause significant alkaline hydrolysis of the silicate network. Typical *in vitro* immersion or cell culture studies using buffered media tend to use glass/solution ratios which keep the pH value well below 9, as the aim is to mimic *in vivo* conditions with their constant fluid exchange.<sup>[73]</sup> This, however, does not take account of the possibility that the pH value may be well above that locally, for example, directly at the glass/solution interface. Silicon-containing species have been detected in solution after immersion of bioactive glasses in both static (Figure 11) and dynamic dissolution experiments,<sup>[61,63,74]</sup> thus showing that dissolution of parts of the silicate network does occur to some extent. It has been suggested that this originates from congruent dissolution of small silicate groups (short chains or rings, which may be present in bioactive glasses) without the need for Si-O-Si hydrolysis,<sup>[23]</sup> but the constant release of significant amounts of silicon species during dynamic dissolution experiments<sup>[66]</sup> together with *in vivo* observations that bioactive glasses can fully degrade<sup>[4a,75]</sup> suggests that hydrolysis of the silicate network does occur.

While network connectivity affects glass degradation,<sup>[66]</sup> solubility and degradation rates can be varied even in glasses

of constant network connectivity. If calcium oxide is systematically replaced by sodium oxide in a bioactive glass, the glass solubility, that is, the rate of ion exchange, has been shown to increase, thereby resulting in a more pronounced pH rise at a given time point during immersion (Figure 12),<sup>[76]</sup> caused by

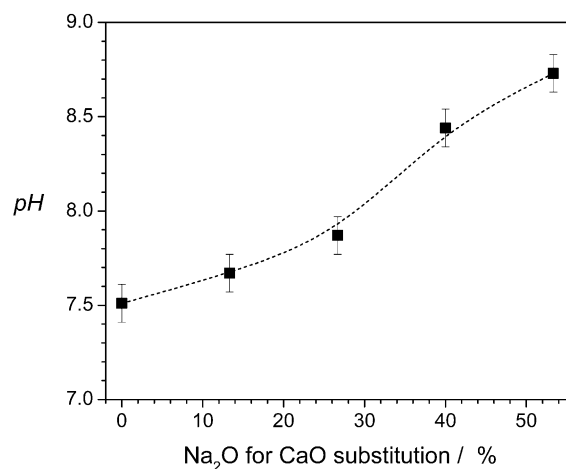


**Figure 12.** pH value of a cell culture medium upon 3 day immersion of bioactive glasses, where CaO was systematically replaced by Na<sub>2</sub>O on a molar basis. Increasing sodium for calcium substitution results in a more pronounced pH rise, caused by faster ion exchange (calculated and plotted from data by Wallace et al.).<sup>[76]</sup>

weaker ionic cross-links because of the lower field strength of sodium ions and a lower packing density.<sup>[52]</sup> This is of interest for bioactive glasses used in degradable polymer composites, as glasses that are too soluble cause fast degradation of the composite material.<sup>[77]</sup> Thus, the use of bioactive glasses with lower alkali metal oxide contents (or alkali-free)<sup>[78]</sup> rather than 45S5 may be preferred for such applications. The substitution of strontium for calcium<sup>[58]</sup> has also been shown to increase glass solubility,<sup>[56]</sup> caused by a lower oxygen packing density<sup>[53a]</sup> as a result of differences in ionic radii.

These results show that altering the solubility of bioactive glass is not only possible through variation of the network connectivity, but also through variation of the type of modifier cation. Together, this potentially allows for tailoring of ion release from bioactive glasses to match clinical requirements.

### 3.2. Apatite Formation

Bioactive glasses, when immersed in physiological solutions, form an apatite surface layer (Figure 13a),<sup>[79]</sup> which is thought to be key for their *in vivo* bioactivity.<sup>[3a,80]</sup>

The term apatite refers to a group of calcium orthophosphates (e.g. hydroxyapatite Ca<sub>5</sub>(PO<sub>4</sub>)<sub>3</sub>OH), which allow for a wide range of substitutions including CO<sub>3</sub><sup>2-</sup> for either OH<sup>-</sup> (A type) or PO<sub>4</sub><sup>3-</sup> (B type), F<sup>-</sup> for OH<sup>-</sup>, or Sr<sup>2+</sup> for Ca<sup>2+</sup>.<sup>[82]</sup> Apatite forms the major component of mineralized human tissue including bone, dentin, and enamel. The apatite in human mineralized tissue, as well as the apatite formed on bioactive glasses immersed in physiological solutions, is

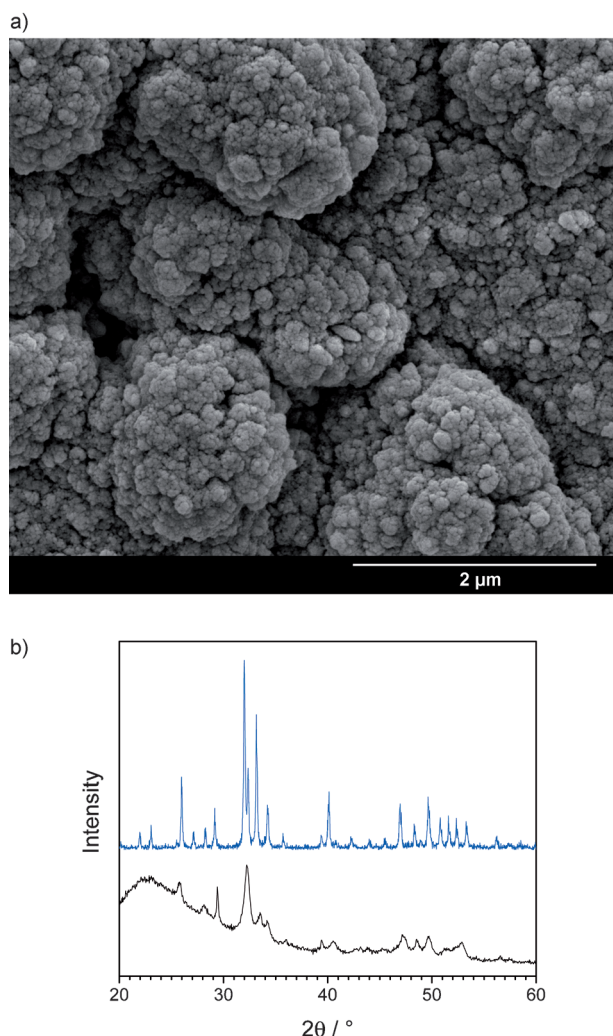


**Figure 13.** a) Scanning electron micrograph showing a fluoride-substituted apatite layer on the surface of a fluoride-containing bioactive glass at 7 days in cell culture medium (RPMI 1640 with 10% fetal bovine serum).<sup>[81]</sup> b) X-ray diffraction patterns of fluorapatite formed by hydrothermal synthesis (blue, top) and by immersing a fluoride-containing bioactive glass in Tris-HCl buffer solution (black, bottom).

usually carbonate-substituted.<sup>[83]</sup> This—in addition to the fact that apatite crystals formed on bioactive glasses has been shown to be in the nanometer size range<sup>[61]</sup> and of poor crystallinity because of various substitutions in the apatite crystal lattice<sup>[63]</sup> (again, similar to bone apatite)—makes bioactive glasses particularly interesting for bone regeneration and may explain the formation of strong interfacial bonds between bioactive glass and bone *in vivo*.<sup>[3a,84]</sup>

Solutions used for the *in vitro* testing of apatite formation vary in their composition. Simulated physiological solutions (simulated body fluid<sup>[85]</sup> (SBF) or cell culture solutions) try to mimic the composition of body fluids and contain relatively high concentrations of phosphate and calcium ions.<sup>[86]</sup> Others, such as Tris-HCl buffer<sup>[63]</sup> or physiological sodium chloride solution,<sup>[87]</sup> do not. The composition of the immersion solution—particularly the presence or absence of ions directly involved in apatite formation, most notably  $\text{PO}_4^{3-}$  and  $\text{Ca}^{2+}$ —clearly plays a role when investigating apatite precipitation

*in vitro*. Many simulated physiological solutions have a composition which is supersaturated with respect to apatite,<sup>[64]</sup> and slight changes in pH or composition can be expected to trigger precipitation. Therefore, even phosphate-free bioactive glasses can form an apatite surface layer in such media.<sup>[80,88]</sup> In solutions such as Tris-HCl buffer, by contrast, all the ions consumed during apatite formation need to be released from the bioactive glass. The presence of a silica gel layer is thought to aid apatite nucleation;<sup>[63,72]</sup> however, other results suggest that it is not a prerequisite for apatite formation, and that apatite therefore may precipitate from solution.<sup>[62,89]</sup> Surface charges and Si-OH groups may indeed still act as nucleation sites for apatite crystallization.<sup>[72,83]</sup>

Experiments using various diffraction methods<sup>[90]</sup> showed that apatite on bioactive glass is actually formed via initial formation of octacalcium phosphate<sup>[91]</sup> and subsequent recrystallization. This agrees with theoretical analysis of phosphate precipitation from SBF, which shows that while hydroxyapatite is the most thermodynamically stable form at pH values between 5 and 10,<sup>[82a]</sup> nucleation rates of octacalcium phosphate are much higher at a physiological pH value. Only when the pH increases do nucleation rates become more similar, being nearly the same at pH 10.<sup>[92]</sup> Distinguishing octacalcium phosphate and apatite by powder X-ray diffraction is complicated by very similar diffraction patterns (in addition to line broadening because of small crystallite sizes, Figure 13b), and the use of additional methods may be necessary to unambiguously identify the various phases.

The apatite-forming ability of glasses has been shown to depend on their network connectivity, with more polymerized glasses showing significantly slower apatite formation (Figure 14a), as a result of less ion release from the glass.<sup>[23b,24]</sup> It has been suggested that the percolation point at a network connectivity of 2.4 represents the cut-off point for apatite formation,<sup>[23a]</sup> as rigid networks do not allow for glass dissolution and significant ion release; however, some glasses with a network connectivity above 2.4 form apatite and are clearly bioactive *in vitro* (e.g. 13-93<sup>[93]</sup> and S53P4,<sup>[71]</sup> Table 1) albeit more slowly than less-polymerized glasses such as 45S5.<sup>[71,94]</sup> If we bear in mind that the network connectivity is an average value only, we can use the network rigidity model to help us understand the bioactivity of more-cross-linked glasses. The presence of floppy regions, which have a lower local network connectivity, will thus allow for water penetration into these regions, thereby resulting in the release of ions and, subsequently, apatite formation. However, as the network connectivity increases, the radii of the floppy regions will become smaller, until apatite formation no longer occurs, and bioactivity is suppressed.

A range of factors have been shown to increase the rate at which apatite is formed. An increase in the phosphate content of bioactive glasses, while maintaining the network connectivity, has been shown to result in a dramatic increase in apatite formation.<sup>[61,89]</sup> Similarly, small additions of fluoride (again, while maintaining network connectivity and polymerization of the silicate structure) have been shown to have a positive effect on apatite formation,<sup>[81,89,95]</sup> most likely through formation of fluorapatite rather than hydroxycarbonate apatite.<sup>[63]</sup> Similarly, substitution of calcium by stron-



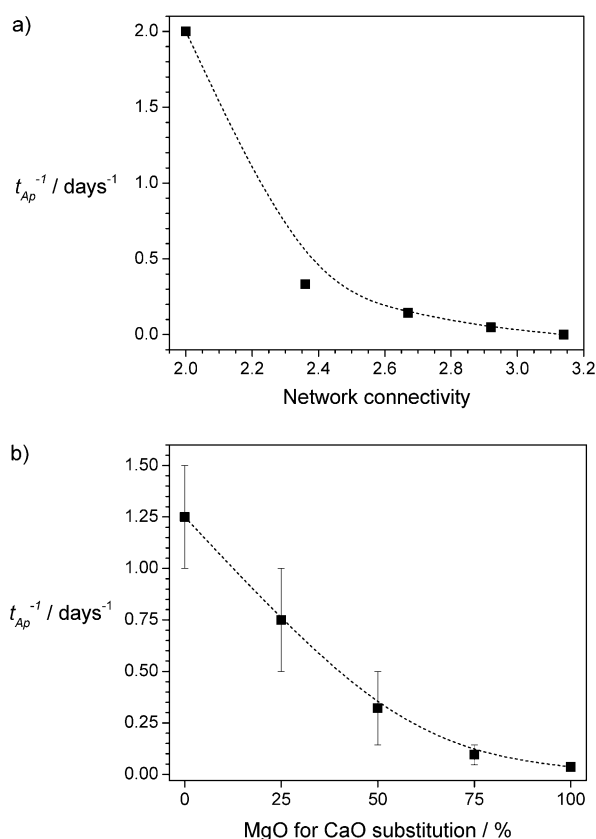


**Figure 14.** Rate of apatite formation ( $t_{Ap}^{-1}$ , where  $t_{Ap}$  is the time of first apatite formation in SBF) of a) phosphate-free  $\text{SiO}_2$ -CaO- $\text{Na}_2\text{O}$  glasses (calculated and plotted from data by Fujibayashi et al.)<sup>[80]</sup> and b) of glass ICIE1 in which calcium is increasingly substituted by magnesium on a molar basis (calculated and plotted from data by Watts).<sup>[80]</sup>

tium has been shown to increase apatite formation through formation of a strontium-substituted apatite,<sup>[56,58]</sup> which shows that ions present in (and released from) the glass can be incorporated into the apatite layer. Despite their lower solubility, alkali metal ion free bioactive glasses have been shown to form apatite no more slowly than alkali metal ion containing ones,<sup>[63,89]</sup> thus suggesting that the presence of alkali metal ions is not a requirement for bioactivity. The explanation is probably that despite a lower overall solubility, the amounts of calcium ions released from the glass (because of higher concentrations of calcium ions present in the glass) are still large enough for the precipitation of apatite.

Serum proteins present in cell culture media have been shown to significantly delay apatite precipitation.<sup>[96]</sup> As body fluids contain various proteins, this may actually more closely reflect the in vivo situation than immersion experiments using protein-free solutions.

The presence of  $\text{Mg}^{2+}$  ions in the immersion medium has also been described to delay apatite formation<sup>[44,97]</sup> through blocking of active growth sites on the crystal surfaces, similar to the action of zinc ions.<sup>[98]</sup> This is interesting as simulated body fluids and cell culture solutions typically contain significant concentrations of magnesium ions. Substitution of calcium by magnesium in bioactive glasses has also been

observed to result in delayed apatite formation (Figure 14b),<sup>[44,99]</sup> and here a dual effect may take place, as substitution of calcium by magnesium has been suggested to increase the silicate network connectivity.<sup>[18]</sup> However, as these glasses also release  $\text{Mg}^{2+}$  ions into the dissolution medium, it is difficult to judge if the delay in apatite formation is caused by the presence of magnesium ions in solution or by reduced degradation and bioactivity of the glass or possibly a combination of both.

As glass structure and ion release affect apatite formation of bioactive glasses, both factors will need to be taken into account when designing new glasses that show fast (e.g. for dental applications) or extremely slow apatite formation (e.g. non-mineralizing glasses for cartilage repair).

### 3.3. Therapeutic Ion Release

In vitro cell culture studies showed that ionic dissolution products from bioactive glasses affect cell proliferation, mineralization, and gene expression,<sup>[100]</sup> and showed that even in the absence of bioactive glass particles a beneficial effect can be detected because of ions released from the glass.<sup>[101]</sup> Glasses are not as dependent on a specific stoichiometry as crystals are, and they allow a larger flexibility in composition. This allows for incorporation of various concentrations of ions with physiological activity and therapeutic properties.<sup>[100]</sup> These ions are released during the dissolution process (Figure 11) and are able to perform their therapeutic action in the human body. In particular, ions acting as modifiers, that is, being ionically linked to nonbridging oxygen atoms, can be released from the glass easily and rapidly by ion exchange with the surrounding body fluid and thus be available in the body. The great advantage of ions locally released from an implant (rather than from systemically administered medication) is that they are released exactly at the site where they are needed, which should result in an optimized therapeutic effect and minimized side effects. Furthermore, bioactive glasses can allow for continued ion release, and thus sustained therapeutic effect throughout glass degradation. As mentioned above, release rates can be adjusted (and thus potentially be optimized) through variation of the glass network connectivity and the type of modifier or intermediate ion. Over the last few years, an increasing number of new bioactive glasses have been developed, most of which focused on incorporating modifier ions with a potential therapeutic benefit.

Calcium ions, which constitute one of the main components of many bioactive glasses and are readily released upon contact of the glass with water, favor osteoblast differentiation<sup>[100]</sup> in addition to favoring apatite precipitation. Strontium-substituted bioactive glasses have been shown to stimulate the bone-forming cells (osteoblasts) while preventing osteoclasts from resorbing bone, similar to strontium-containing drugs for treating osteoporosis.<sup>[102]</sup> Silver ions are well known to exhibit antibacterial properties,<sup>[103]</sup> and owing to their charge to size ratio being similar to that of sodium ions, they can be incorporated into glasses by ion exchange with a molten silver salt.<sup>[104]</sup> The similarity between  $\text{Ag}^+$  and

$\text{Na}^+$  results in a similar release behavior, with fast release of silver ions<sup>[105]</sup> allowing for antibacterial action.<sup>[106]</sup>

Fluoride-containing bioactive glasses<sup>[107]</sup> are of interest for dental applications to prevent dental caries,<sup>[108]</sup> as fluoride-releasing bioactive glasses have been shown to form fluorapatite in physiological solutions,<sup>[63,89]</sup> which is more stable against acid attack than hydroxycarbonate apatite. In addition, fluoride is efficacious in promoting bone formation and preventing osteoporosis-related fractures when administered at appropriate doses,<sup>[109]</sup> and, thus, fluoride-releasing bioactive glasses may potentially be used for bone-regenerating applications.<sup>[81]</sup> In bioactive glasses, fluoride ions complex modifiers such as sodium or calcium,<sup>[38,42c]</sup> and the large electronegativity of fluorine leads to a more ionic character of the chemical bonds,<sup>[21]</sup> with the fluoride part of the glass structure showing some similarity to that of fluorite. However, unlike the low solubility of fluorite, bioactive glasses readily release calcium and fluoride ions,<sup>[63,95a]</sup> at least until a fluorapatite surface layer reduces ion release, thus acting as a protective layer.<sup>[81]</sup>

Zinc-containing bioactive glasses<sup>[48,110]</sup> have been developed, as zinc ions are known to be bactericidal and essential for wound healing.<sup>[111]</sup> However, appropriate release levels of zinc ions have to be maintained, as high concentrations of zinc have been shown to be cytotoxic.<sup>[112]</sup> One interesting property of zinc-containing bioactive glasses is that only small amounts of zinc ions are released under normal physiological pH conditions (pH 7.4),<sup>[48,113]</sup> while zinc release increased dramatically under acidic conditions.<sup>[48]</sup> This indicates that the release mechanism for intermediate ions may be more complicated than the simple ion exchange observed for modifier ions. It has been suggested that the release mechanism is strongly pH dependent, with zinc being involved at low pH values through acid hydrolysis of Si-O-Zn bonds, but not at a neutral pH.<sup>[48]</sup> As low pH conditions are present during inflammation or bacterial infection, zinc-releasing bioactive glasses may potentially be used as release devices, which release  $\text{Zn}^{2+}$  and perform bactericidal action only when needed.<sup>[48]</sup> Magnesium ions have been incorporated into bioactive glasses, as they are known to stimulate new bone formation despite impeding apatite crystallization in vitro.<sup>[44,100]</sup> Magnesium-containing glasses may possibly show a similar release mechanism as zinc-containing ones, as the presence of potentially acid hydrolyzable Si-O-Mg bonds has been suggested by  $^{29}\text{Si}$  MAS NMR experiments.<sup>[114]</sup>

Vascularization is a critical step during tissue regeneration, as cell proliferation depends on the supply of oxygen and nutrients. Angiogenesis, that is, the formation of new blood vessels, is activated by a low oxygen pressure (hypoxia) pathway,<sup>[115]</sup> and bioactive glasses have been suggested to stimulate angiogenesis.<sup>[116]</sup> Cobalt-substituted bioactive glasses showed cobalt ions to partially enter the silicate network, similar to other intermediates such as magnesium or nickel.<sup>[51]</sup> The glasses showed a controlled release of cobalt ions within a therapeutically active concentration range, which suggests that they might potentially be used as new hypoxia-mimicking materials for regenerative medicine.<sup>[115]</sup> Copper<sup>[117]</sup> and nickel-containing<sup>[51]</sup> bioactive glasses have been investigated for the same purpose.

The release of network formers has also been shown to affect cells in vitro. As discussed in Section 3.1, silicon species are released from bioactive glasses through a combination of alkaline hydrolysis and congruent release of small silicate species such as short chains or rings. As condensation of silanol groups occurs readily, resulting in formation of a silica gel layer,<sup>[118]</sup> actual concentrations of silicon-containing species in solutions remain relatively low.<sup>[63]</sup> Nonetheless, silicon ions have been suggested to be one of the key factors causing the bioactivity of glasses<sup>[119]</sup> and stimulating osteoblast differentiation.<sup>[101]</sup> Borate glasses are gaining increasing interest as biomaterials,<sup>[120]</sup> and borate-containing bioactive silicate glasses have been investigated for many years,<sup>[9]</sup> and the release of boron has been suggested to stimulate RNA synthesis in fibroblasts.<sup>[100]</sup>

## 4. Crystallization and Processing

### 4.1. Crystallization Tendency

Many bioactive glasses have a high tendency to crystallize<sup>[121]</sup> either during preparation, thereby making it challenging to actually obtain the glass in an amorphous state,<sup>[36,122]</sup> or during further processing at high temperatures.<sup>[123]</sup> One reason for this pronounced devitrification tendency is their highly disrupted silicate network of low network connectivity. The large concentration of nonbridging oxygen atoms reduces the covalent cross-linking between the silicate chains, thereby resulting in an increased mobility of the structural units which facilitates rearrangement to form critical size nuclei. As described by the network rigidity theory, below a network connectivity of 2.4 the whole network can be described as floppy, thereby allowing for nucleation and, thus, crystallization to occur anywhere in the network. For glasses with higher network connectivity, nucleation can be expected to occur in the floppy areas first.<sup>[26]</sup>

It should, therefore, be expected that the crystallization behavior varies with network connectivity, and indeed pronounced differences have been detected between 45S5 (with its low network connectivity, Table 1) and more polymerized glasses, such as S53P4.<sup>[40,124]</sup> There have been indications that bioactive glasses crystallize by a surface mechanism;<sup>[37,124]</sup> however, while some glasses indeed show surface crystallization<sup>[125]</sup> (e.g. S53P4),<sup>[40]</sup> the mechanism for 45S5 is more complicated, possibly because of phase separation.<sup>[39,40]</sup> This resulted in 45S5 showing bulk or surface crystallization if particle size<sup>[40,126]</sup> or heat-treatment regime<sup>[125]</sup> were varied.

A simplified approach for describing the ability of glasses to be processed at high temperatures without crystallization occurring is by calculating the temperature difference between crystallization<sup>[127]</sup> and the glass transition.<sup>[128]</sup> This processing window,  $\Delta T$ , is the temperature range in which glass viscosity allows for sintering, fiber drawing, or other processing. It has been shown to widen with increasing polymerization of the silicate network (Figure 15a), thus illustrating that more polymerized glasses are less prone to crystallization.

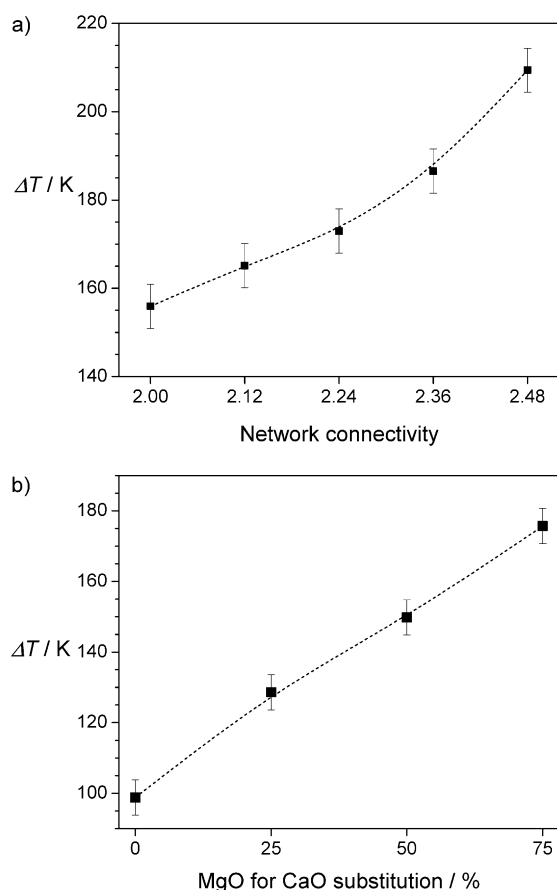


**Figure 15.** Increase in the processing window ( $\Delta T$ , temperature range between glass transition and crystallization) with a) increasing network connectivity (glasses based on 45S5, network connectivity 2.11) and b) increasing substitution of calcium by magnesium in glass ICIE1 (calculated and plotted from data presented by Watts et al.).<sup>[18,114]</sup> A larger processing window facilitates sintering or fiber drawing without crystallization occurring.

The network connectivity, however, is not the only parameter affecting crystallization. The devitrification tendency has been shown to increase with an increasing ratio of alkali/alkaline earth metal cations in the glass.<sup>[129]</sup> Arstila et al. showed that bioactive glasses can be divided into two main groups, those crystallizing to sodium calcium silicates (such as combeite,  $\text{Na}_2\text{O}-2\text{CaO}-3\text{SiO}_2$ ) and those crystallizing to wollastonite ( $\text{CaO}-\text{SiO}_2$ ),<sup>[124,130]</sup> with the latter showing a significantly increased processing window (300 K compared to around 100 K).<sup>[131]</sup> This shows that bioactive glasses, such as 45S5, with high contents of low field strength alkali metal ions are disadvantageous for processing, while glasses with low contents, such as 13-93, are preferred.

Bioactive glasses with higher phosphate contents (around 6 mol %) have been shown to crystallize to phosphate (rather than silicate) phases, such as sodium calcium orthophosphates for glasses with high alkali oxide contents<sup>[36,122]</sup> and apatites for alkali metal oxide free glasses.<sup>[36,128]</sup> In particular, fluoride-free high phosphate content bioactive glasses seemed to show spontaneous crystallization of phosphate phases.<sup>[36]</sup> These results show that while high phosphate contents are beneficial

for apatite formation in physiological solutions,<sup>[61,89]</sup> these glasses may be more difficult to process.

It is interesting to note that it is actually possible to maintain an amorphous orthophosphate environment in bioactive phosphosilicate glasses. In (silicate-free) phosphate glasses, the crystallization tendency is known to increase with shorter phosphate groups,<sup>[132]</sup> and glasses containing orthophosphate groups are, in particular, very difficult to obtain in an amorphous state by using conventional melt-quench techniques, unless significant amounts of intermediate oxides are present.<sup>[133]</sup> In low-phosphate-content bioactive phosphosilicate glasses, the phosphate-rich regions may possibly be too small to allow for nucleation and crystallization of orthophosphate species, while in high phosphate compositions they are not, resulting in spontaneous crystallization of these phases.

The crystallization tendency of glasses can also be advantageous, and it has been used to prepare bioactive glass-ceramics.<sup>[128,134]</sup> Here the glass is subjected to a controlled temperature treatment, which results in the crystallization of selected phases such as apatite, wollastonite, or phlogopite,<sup>[135]</sup> and some of these materials have been used with great success commercially (e.g. Cerabone and Bioverit).

#### 4.2. How To Avoid Crystallization

If both bioactive glasses and glass-ceramics<sup>[135a]</sup> can be used successfully in vivo, why is it so important to avoid glass crystallization? Crystallization (or partial crystallization) has been reported to affect the bioactivity of bioactive glasses such as 45S5, with bioactivity decreasing significantly with increasing temperature during heat treatment.<sup>[136]</sup> Magallanes-Perdomo et al. explained these changes by increasing percentages of crystalline (sodium calcium silicate) phase being present in the glass, which increased the network connectivity of the remaining glass phase as the heat was increased.<sup>[137]</sup> However, we need to distinguish between different glass compositions. While bioactive glasses of low phosphate content crystallize to silicate phases,<sup>[40,134a,137]</sup> glasses with high phosphate content crystallize to phosphate phases, including apatite,<sup>[36,122,128]</sup> and glass-ceramics containing apatite as a main crystal phase (e.g. Cerabone and Bioverit)<sup>[85,135b]</sup> have been shown to be highly bioactive. Therefore, partial crystallization will not necessarily reduce the bioactivity, depending on the crystal phases forming and the composition of the remaining glass phase.

One of the main advantages of glasses is, however, that they can easily be processed into various shapes (e.g. fibers)<sup>[12]</sup> or be sintered (e.g. into porous scaffolds or coatings), and the presence of crystals can have a negative impact on processing. They are detrimental during fiber drawing, as they can cause fiber breakage during the drawing process. In addition, bioactive glasses often crystallize by a surface nucleation mechanism,<sup>[40]</sup> which tends to inhibit sintering by a viscous flow mechanism.<sup>[123]</sup> Therefore, to effectively process a bioactive glass, its crystallization tendency needs to be controlled.

The easiest way to reduce the crystallization tendency of bioactive glasses is to increase their network connectivity



(Figure 15 a). Indeed, bioactive glasses known for their good processing, such as 13-93<sup>[9]</sup> (Table 1), have a higher network connectivity than Hench-type bioactive glasses such as 45S5.<sup>[3a]</sup> As an increase in network connectivity is likely to reduce the solubility and bioactivity, however, this approach can be counterproductive.

A slightly different approach is the incorporation of another network former such as B<sub>2</sub>O<sub>3</sub>,<sup>[138]</sup> as in bioactive glass 1-98.<sup>[124,138b]</sup> Bioactive borate glasses (some of which are SiO<sub>2</sub>- and P<sub>2</sub>O<sub>5</sub>-free, while others actually contain certain amounts of SiO<sub>2</sub> or P<sub>2</sub>O<sub>5</sub>) have been reported<sup>[120a,139]</sup> to perform comparably well in vitro and in vivo as typical phosphosilicate bioactive glasses.<sup>[120b]</sup> As a consequence of the complicated structural behavior of B<sub>2</sub>O<sub>3</sub> in the glass, including both BO<sub>3</sub> and BO<sub>4</sub> units depending on the composition,<sup>[12]</sup> processing seems to vary with B<sub>2</sub>O<sub>3</sub> content in the glass, and glasses with BO<sub>3</sub> units exclusively showed improved processing in particular.<sup>[138a]</sup> However, although bioactive boron-containing silicate glasses have been investigated for years,<sup>[129]</sup> more systematic studies are needed to help us fully understand how to use B<sub>2</sub>O<sub>3</sub> to improve the processing of bioactive glass.

Even while maintaining the network connectivity, the processing behavior can be improved by varying the network modifiers. Reduction of the alkali/alkaline earth metal oxide ratio was shown to improve the processing of bioactive glasses.<sup>[124]</sup> Based on this knowledge, several glasses have been developed that show improved processing,<sup>[140]</sup> including low alkali metal oxide content glasses 13-93<sup>[9]</sup> and ICIE16<sup>[11,141]</sup> and alkali metal oxide free compositions.<sup>[78b]</sup> The mixed-alkali effect is also known to improve the processing of glasses,<sup>[57]</sup> and it has been shown to improve the processing of bioactive glasses through lowering the glass transition temperature, increasing the crystallization temperature, and thereby widening the processing window.<sup>[32b]</sup> In addition, the processing of highly disrupted glasses can be improved by increasing the number of glass components, which has been suggested to increase the entropy of mixing and impede crystallization through a higher energy barrier for atomic rearrangement to form critical size nuclei.<sup>[142]</sup>

Another approach for improving glass processing is the incorporation of intermediate ions such as magnesium,<sup>[44,99,128]</sup> which because of their larger field strength compared to modifiers<sup>[41a]</sup> effectively widen the processing window (Figure 15b).<sup>[18]</sup> It has also been suggested that when magnesium becomes incorporated into the silicate structure of a glass, it may act in an analogous fashion to co-monomers in organic polymers to suppress crystallization.<sup>[142a]</sup> Composition 13-93 is a well-known example of a magnesium-containing bioactive glass with a low crystallization tendency. However, if magnesium enters the silicate network it also increases the network connectivity, and therefore the bioactivity may be expected to decrease.<sup>[114]</sup>

Ultimately, a balance will always have to be found between crystallization on the one hand and bioactivity on the other. Improving the processing of bioactive glasses while maintaining a high bioactivity is likely to remain a challenge.

### 4.3. Processing of Bioactive Glasses

Bioactive glasses can be sintered into *porous scaffolds* (which have recently been reviewed in detail by Rahaman et al.<sup>[139]</sup> and Jones)<sup>[94]</sup> by various processes including gel-cast foaming (Figure 16c),<sup>[141]</sup> foam replica templates,<sup>[143]</sup> and salt sintering techniques.<sup>[144]</sup> One major drawback of porous bioactive glass scaffolds is their poor strength. While glasses are inherently brittle,<sup>[145]</sup> the mechanical properties of bioactive glass scaffolds can be significantly improved by changing the scaffold architecture through unidirectional freezing<sup>[146]</sup> or rapid prototyping,<sup>[147]</sup> reaching compressive strengths in the range of cortical bone (100 to 140 MPa).<sup>[139,148]</sup>

Porous bioactive glass scaffolds having an open, interconnected porous structure mimicking that of cancellous bone (Figure 16c)<sup>[149]</sup> are of interest for use as bone fillers for in situ bone regeneration, as they allow for cell ingrowth while the material degrades to be replaced with new bone<sup>[15b]</sup> and can release modifier ions with therapeutic benefits.<sup>[100]</sup> Porous scaffolds are also being investigated for tissue engineering applications, where a scaffold is seeded with cells ex situ before being implanted.<sup>[150]</sup> In both cases, pore diameters and connections need to be large enough to allow cells, tissue, and blood vessels to penetrate the structure. Furthermore, the scaffolds need to allow for cell attachment and proliferation as well as guide tissue growth.<sup>[15b]</sup> To maintain scaffold properties such as mechanical strength and bioactivity, crystallization needs to be controlled during sintering. This is the reason why many studies used glasses such as 13-93<sup>[146,147]</sup> or ICIE16,<sup>[141]</sup> which are known for their improved processability. Scaffolds prepared from 45S5, by contrast,

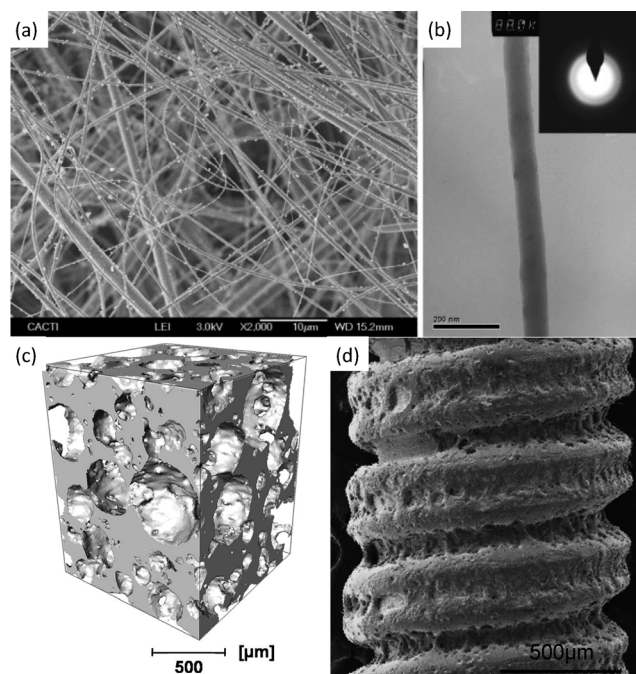


**Figure 16.** a,b) Bioactive glass nanofibers prepared by laser spinning,<sup>[157]</sup> c) an X-ray microtomography (μCT) image of a bioactive glass scaffold prepared by gel-cast foaming (reproduced from Wu et al.<sup>[141]</sup> with permission from Elsevier) and d) Ti6Al4V dental implant with bioactive glass coating prepared by enameling.<sup>[142a]</sup>

tend to be partially or even fully crystalline<sup>[143]</sup> because of its high crystallization tendency.<sup>[123]</sup>

*Bioactive glass fibers* are of interest as cotton wool like bone-void fillers,<sup>[151]</sup> fiber mats for soft tissue repair,<sup>[152]</sup> or for reinforcing resorbable polymers.<sup>[153]</sup> Metaphosphate glasses, consisting of a structure of long ( $Q^2$ ) phosphate chains, have been shown to exhibit anisotropic properties<sup>[154]</sup> when extruded or drawn into fibers because of the alignment of the phosphate chains along the fiber axis.<sup>[155]</sup> A similar behavior may possibly be expected for bioactive glasses with their large fraction of  $Q^2$  groups. However, many of these compositions (such as 45S5) cannot be drawn into fibers by using conventional fiber drawing techniques because of their pronounced crystallization tendency.<sup>[93,156]</sup> The only way to address this is through the glass composition, thus making the glass less prone to crystallize or by using alternative approaches for fiber making. Recently, cotton-wool-like 45S5 fibers have been prepared successfully by laser spinning (Figure 16a,b),<sup>[157]</sup> a method which allows for fast cooling rates that inhibit crystallization. Melt spinning also allows for fast cooling rates, and while this technique has been successfully used to make 13-93 glass fibers,<sup>[158]</sup> it may even be appropriate for glasses with higher crystallization tendencies, such as 45S5, thus allowing the preparation of fiber mats, for example, for wound-healing applications.

Implants for load-bearing applications are usually made from metals such as Ti6Al4V or Co-Cr alloy.<sup>[2a]</sup> *Bioactive coatings* (often plasma-sprayed hydroxyapatite)<sup>[159]</sup> are deposited on the implant to improve bioactivity and osseointegration of these implants so as to provide a strong bond between the prosthesis and bone. One early intended application of Hench's Bioglass was for coating the femoral stem of hip prostheses for cement-free fixation in the bone,<sup>[160]</sup> and the procedure involved dip coating the prosthesis in the molten liquid glass at very high temperatures.<sup>[161]</sup> The use of bioactive glass coatings may, however, be more suitable for smaller implants (e.g. dental implants) rather than hip prostheses, and may require porous implant surfaces to provide mechanical interlocking in addition to bonding between coating and bone to ensure long-term mechanical performance.

The preparation of sintered glass coatings on metals (known as enameling) is an old and well-understood technique, and therefore sintered bioactive glass coatings (Figure 16d) are promising candidates to improve the bioactivity of metallic implants. The requirements, however, are numerous, and include a low tendency of the glass to crystallize during sintering, a thermal expansion coefficient matched to that of the metal substrate,<sup>[162]</sup> good mechanical adhesion and performance, and high bioactivity. Matching the thermal expansion is particularly challenging, as owing to their high modifier and particularly sodium contents, typical bioactive glasses tend to have thermal expansion coefficients too high to allow for the use as coatings.<sup>[10]</sup> Recent approaches included graded coatings<sup>[10,163]</sup> with a non-bioactive innermost layer of high network connectivity (3.05; glass 6P61, Table 1) that showed a thermal expansion coefficient matched to that of Ti6Al4V alloy,<sup>[10]</sup> while the outermost layer had a lower network connectivity (2.36; glass 6P50, Table 1) that allowed for in vitro apatite formation<sup>[164]</sup> and cell proliferation.<sup>[163a,165]</sup>

An additional glass layer of intermediate properties was sandwiched between those two layers.<sup>[10]</sup> In another recent approach, a glass having a low network connectivity (for bioactivity) while containing intermediate oxides and a low alkali/alkaline earth metal oxide ratio (for reducing the thermal expansion coefficient) was developed as a single-layer implant coating (Figure 16d).<sup>[142a]</sup>

Taken together, the processing of bioactive glasses shows that changes in glass composition, and thus structure, can improve glass processing. In addition, however, variation of other parameters such as the processing method,<sup>[148a]</sup> particle size ranges,<sup>[166]</sup> or the use of additives may be necessary to obtain the desired results.

## 5. Bioactivity of Glasses

### 5.1. In Vitro Bioactivity

Simple immersion tests in simulated physiological solutions, while giving insight into glass dissolution and apatite formation, cannot predict the actual in vivo bioactivity of a material.<sup>[64]</sup> The testing solutions used are compositionally simple and are usually devoid of proteins such as collagen, fibronectin, or vitronectin,<sup>[167]</sup> which have been shown to affect apatite formation on bioactive glasses<sup>[96]</sup> and cell (e.g. osteoblast) adhesion<sup>[167]</sup> on the apatite surface (Figure 17). In vitro cell tests, by contrast, are usually performed using culture media containing serum proteins in addition to physiological ionic concentrations. They allow for testing the influence of a bioactive glass (its ion release, apatite formation, and other factors such as surface topography) on living cells by growing the cells in direct contact with the glass. Alternatively, the influence of its dissolution products only is assessed using indirect methods.<sup>[100]</sup>

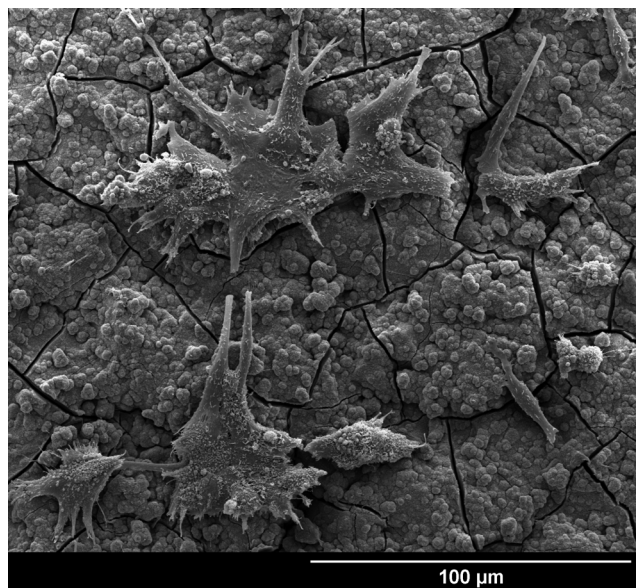


**Figure 17.** Scanning electron micrograph showing osteoblasts on an apatite surface layer formed on a bioactive glass. (The surface cracks were caused by dehydration of the apatite layer for SEM analysis.)

Bioglass 45S5 has been shown to stimulate cell cycling in vitro, which results in faster osteoblast turnover and, as a consequence, a more mature cell population capable of producing mineralized tissue within a relatively short time.<sup>[73]</sup> Experiments using the dissolution products of 45S5 showed that osteoblast proliferation was increased by gene upregulation. This is most likely caused by ions released from the glass,<sup>[101]</sup> which is interesting, particularly for tissue engineering applications, as it suggests that supplementation with growth factors is not needed for bioactive glasses unlike for other bioceramics. Experiments using rodent mesenchymal stem cells showed increased osteoblastic differentiation when grown on 45S5, while human mesenchymal stem cells did not,<sup>[168]</sup> thereby demonstrating that results from cell culture experiments are not only affected by the substrate used but also by the cell type.

In vitro cell tests have shown an influence of the glass network connectivity on cell proliferation, with more polymerized glasses (e.g. glass 6P55, Table 1) showing lower cell proliferation than less polymerized ones (glass 6P50),<sup>[165]</sup> in agreement with predictions by acellular immersion tests. This effect is most likely to be explained by a range of factors, including slower apatite formation (thereby reducing protein adsorption and initial cell attachment)<sup>[167]</sup> and reduced ion release (including calcium and silicon ions, which are known to stimulate osteoblast proliferation and differentiation)<sup>[100]</sup> for the more polymerized glasses.

Apart from the silicate network polymerization, modifiers present in (and potentially released from) bioactive glasses can have a pronounced effect on cell proliferation and differentiation. Strontium-substituted bioactive glasses have been shown to combine the known beneficial effects of bioactive glasses on bone regeneration with the ability of released strontium ions to stimulate bone formation by osteoblasts while inhibiting osteoclastic bone resorption. This property makes them potential candidates for bone regeneration in patients suffering from osteoporosis.<sup>[102a]</sup> More importantly, however, these studies demonstrated the beneficial effects of incorporating therapeutically active ions in a surface-active material such as bioactive glasses.<sup>[102b]</sup> It is worth noting that in the studies cited, the network connectivity was maintained constant through molar substitutions of calcium by strontium. This allowed the influence of strontium substitution to be tested without influences resulting from changes to the silicate polymerization.

Results on fluoride-containing bioactive glasses showed, again, the importance of glass design. Findings have been somewhat contradictory, either showing beneficial effects on cell proliferation and bone mineralization<sup>[81]</sup> or toxic responses through oxidative cell damage.<sup>[169]</sup> However, in the first study the glass network connectivity was kept constant,<sup>[81]</sup> while in the second it was not,<sup>[169]</sup> which resulted in decreased apatite formation in the second study.<sup>[62]</sup> This may suggest that a combination of factors (including apatite formation in addition to fluoride release) is necessary for optimum performance of fluoride-releasing bioactive glasses.

Bioactive glasses have exhibited antibacterial effects in vitro, caused by a rise in the pH value in the surrounding medium as a result of ion exchange.<sup>[170]</sup> They can significantly

reduce cell counts of bacteria involved in implant-related infections such as *Staphylococcus aureus* or *Staphylococcus epidermidis*, but also bacteria known for their role in caries (*Streptococcus mutans*) or in periodontal disease (*Porphyromonas gingivalis*).<sup>[171]</sup> Silver-containing bioactive glasses<sup>[104]</sup> are of particular interest, as the release of silver ions with their well-known antibacterial properties<sup>[103]</sup> can be expected to improve the antibacterial properties of bioactive glasses even further. This is particularly interesting, as bioactive glasses releasing bactericidal ions (such as silver or zinc ions) would not require a pronounced rise in the pH value for bactericidal effects, as too high a pH rise can also be detrimental to cells.

## 5.2. In Vivo Bioactivity

While in vitro cell culture experiments offer several advantages over acellular immersion tests, they still have certain limitations. For example, cell tests are usually performed in a closed or static system, which can lead to a build-up of high ionic concentrations, while fluid transport avoids this in a living organism. In vivo tests, therefore, allow us to predict the clinical performance of a bioactive glass better.

In vivo studies in rabbits showed that 45S5 particles led to faster bone formation than synthetic hydroxyapatite particles<sup>[172]</sup> and, unlike apatite, also completely degraded over time,<sup>[173]</sup> thus allowing for bone regeneration.<sup>[4a]</sup> This degradation was suggested to be caused by a dissolution process, caused by initial ion exchange resulting in a silica-gel layer,<sup>[174]</sup> rather than being cell-mediated, and the glass particle dissolution correlated with bone formation.<sup>[172]</sup>

Fujibayashi et al. investigated the influence of silicate polymerization on in vivo performance, and they implanted bioactive glasses of varying network connectivity into the femoral condyles of rabbits. Their results agreed well with those of immersion tests performed simultaneously in simulated body fluid,<sup>[80]</sup> with increasing network connectivity showing significantly slower apatite formation in vitro (Figure 14a) as well as significantly reduced bone formation in vivo (Figure 18). In addition, glasses with low network connectivities degraded in vivo, while those with high network connectivities did not show signs of degradation.<sup>[80]</sup> This finding is in agreement with in vitro dissolution studies showing significantly lower glass dissolution for more polymerized silicate glasses.<sup>[66]</sup> Similarly, Strnad<sup>[24b]</sup> reported excellent osseointegration within 2 months for glasses with network connectivities of 2.11 (45S5) and 2.51, while more polymerized glasses (network connectivities of 3.32 and 3.83) showed fibrous tissue encapsulation only.<sup>[175]</sup> This shows that if the differences in network connectivity are small, glasses may give comparable results in vivo, despite differences in vitro. Results by Hupa et al. confirmed this by showing slower apatite formation of glass S53P4 in simulated body fluid compared to 45S5, while the reaction layers formed on specimens implanted into rat muscle showed no significant differences (Figure 19).<sup>[171]</sup>



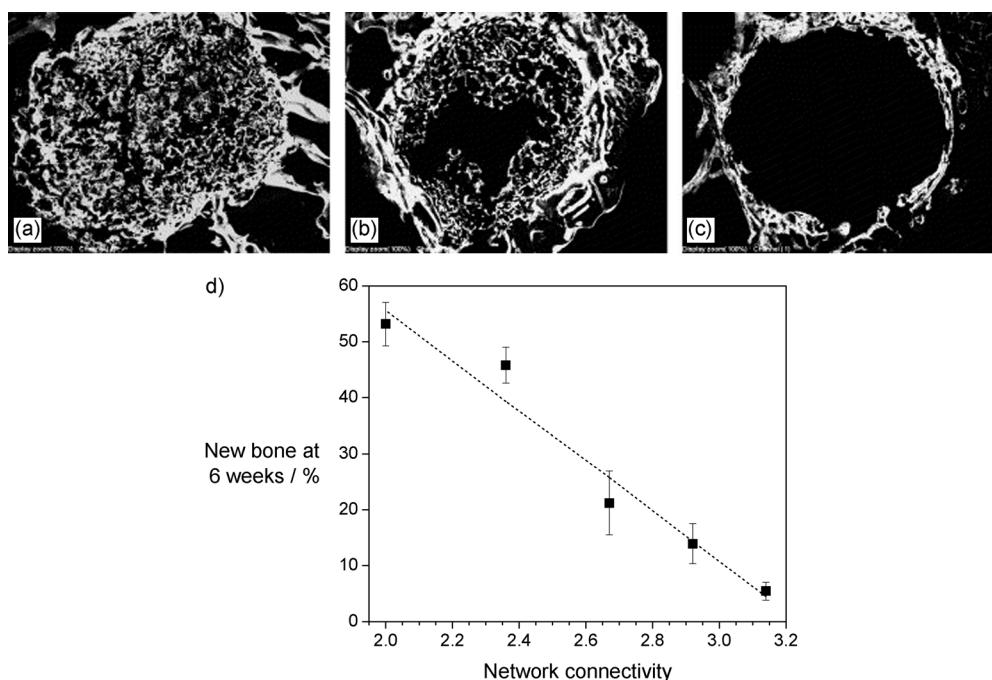


**Figure 18.** Histomorphological results showing newly formed bone labeled with fluorescent calcein at 6 weeks after implantation of  $\text{SiO}_2\text{-CaO-Na}_2\text{O}$  glasses with a network connectivity of a) 2, b) 2.6, and c) 3.1 (the diameter of circular area is 6 mm). (Reproduced from Fujibayashi et al.<sup>[80]</sup> with permission from Pergamon.) d) Percentage of calcein-labeled newly formed bone at 6 weeks in vivo (calculated and plotted based on data presented by Fujibayashi et al.).<sup>[80]</sup> Significantly less new bone is formed as the network connectivity increases.

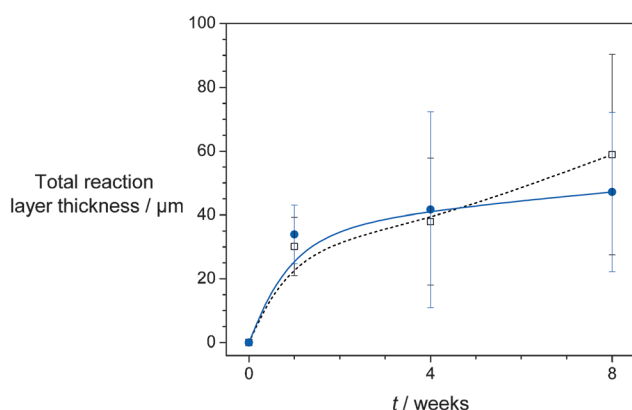


**Figure 19.** Total thickness of the reaction layer (silica-rich and apatite) at 1, 4, and 8 weeks of implantation of glasses 45S5 (black squares) and S53P4 (blue circles) in rat muscle. (Plotted from data presented by Hupa et al.)<sup>[71]</sup>

### 5.3. Clinical Studies

Bioglass 45S5 was originally developed as a bone replacement material,<sup>[5a]</sup> and its first use as an implant was as a replacement for damaged bone tissue, for example, as middle ear prostheses<sup>[176]</sup> and for orbital floor reconstruction.<sup>[177]</sup> In these first applications, monolithic devices, either custom-made for each individual patient or of standard (e.g. conical) shape, were used. Monoliths were also used as alveolar fillings after tooth extraction,<sup>[178]</sup> with the aim of delaying the resorption of alveolar ridges. After animal

studies had shown that bioactive glasses degrade while stimulating the formation of new bone,<sup>[4a,75]</sup> interest grew in the use of bioactive glasses to regenerate bone. Implant studies in alveolar sockets showed that bioactive glass particles degraded over time,<sup>[179]</sup> with resorption rates being significantly faster than for demineralized freeze-dried bone allograft.<sup>[4b]</sup>

Long-term studies on BonAlive S53P4 showed that the glass is well tolerated in children<sup>[180]</sup> and adults,<sup>[181]</sup> allowing for bone remodeling, vascularization, and cartilage repair. It also showed antibacterial properties.<sup>[182]</sup> Despite glass degradation (and thus the release of glass components into the body) silicon concentrations in patients with S53P4 implants were no higher than for those with autogenous bone implants.<sup>[183]</sup> The structural differences between 45S5 and S53P4 (network connectivity 2.11 and 2.54, respectively; Table 1) do not seem to result in any differences in how well the glasses are tolerated in the human body. However, defect size and the glass particle size fraction used had an effect on degradation rates, with six out of eight large bone defects (size given as ellipsoidal volume;  $23.4/28.8\text{ cm}^3$ ) after tumor removal was filled with particles of various size ranges (1–2, 2–3, or 3.15–4 mm) still showing S53P4 remnants in patients 14 years after implantation, while none were observed in small defects ( $1.1/2.3\text{ cm}^3$ ; particles 1–2 mm).<sup>[181]</sup> No information was given on the exact particle size range in the large defects, thus making it difficult to judge if particle size, defect size, or a combination of both caused the delay in degradation. However, as animal studies showed an influence of particle size,<sup>[4a]</sup> it is likely that it was the larger particles which remained.

The number of bioactive glass compositions which have been tested clinically is small, and no information is available on the influence of systematic compositional changes on bioactive glass compatibility in humans. A strontium-substituted version of 45S5 (StronBone, 10% of the calcium replaced by strontium compared to 45S5;<sup>[102b]</sup> particle size range 0.1–0.8 mm)<sup>[184]</sup> has recently been shown to not only show extensive new bone formation but also significant degradation within three months of implantation into the alveolar socket of an adult.<sup>[184]</sup>

The ability of bioactive glasses to form apatite is not only of benefit for bone regeneration. As apatite forms the inorganic component not only of bone but also of teeth (enamel, dentin, and cementum), bioactive glasses may also to some extent help to regenerate tooth tissue. Enamel can be remineralized if the damage caused by caries or acid erosion is small,<sup>[185]</sup> and the process can be supported by ions released from dentifrices (containing high concentrations of phosphate and calcium and often also fluoride ions) but also from a bioactive glass. The first commercial use of a bioactive glass in oral health has been for the treatment of dentin hypersensitivity,<sup>[186]</sup> with the aim of occluding<sup>[187]</sup> exposed dentinal tubules, which are thought to be the cause of this common pain syndrome,<sup>[187]</sup> through apatite formation. More recently, the potential of bioactive glass as a remineralizing agent for teeth has also been recognized.<sup>[186, 188]</sup> Another commercial application of bioactive glass in the dental field includes the use as an abrasive agent for the polishing of teeth by air abrasion.<sup>[189]</sup>

So far, only the 45S5 composition has been used in oral health applications, but it has been suggested that it may actually be too hard and thus too abrasive for use in dentifrices.<sup>[190]</sup> This highlights the need for new bioactive glasses with lower hardness through a lower network connectivity or additional components such as fluoride or chloride.<sup>[191]</sup>

## 6. Summary and Outlook

Bioactive glasses degrade in physiological solutions and form a surface layer of biomimetic apatite, thus allowing for the formation of a strong bond to bone and enabling bone regeneration rather than just bone replacement. Their ability to do this depends strongly on their structure, with both the polymerization of the silicate network and the phosphate environment being critical for bioactive glass performance in vitro and in vivo. In addition, bioactive glasses allow for the incorporation and the subsequent controlled release of physiologically active ions, thereby providing additional therapeutic benefits for, among others, bone regeneration, bactericidal action, or vascularization.

However, their commercial success is not as great as one might expect based on their excellent biocompatibility and bioactivity, and the reason is likely to be the fact that clinical applications have so far been limited to particulate bioactive glass, which is only suitable for non-load-bearing applications. Hopefully their range of uses can be extended significantly as new bioactive glass products are developed, which combine

bioactivity and mechanical strength with ease of use and, ideally, allowing for minimally invasive application.

To successfully develop new compositions, however, it is necessary for researchers to take a more structural approach when designing bioactive glasses. In particular, molar substitutions, based on a thorough understanding of the structural role of each component in the glass, allow for incorporation of new components without altering the silicate structure and thus the overall reactivity of the glass.

*I wish to thank my current and former students, Maxi Tylkowski, Steffen Müller, Liane Bingel, Marcus Abend, and Daniel Groh, for providing some unpublished experimental data. I further wish to express my deep gratitude to Dr. Natalia Karpukhina, Queen Mary, University of London, for countless fruitful discussions over the years, her insightful comments during preparation of this manuscript, and her loyal friendship. The MD simulation of a bioactive glass structure shown in the cover image has been reproduced from a publication by Xiang and Du,<sup>[16b]</sup> and the porous scaffold from a publication by Wu et al.<sup>[141]</sup> (with permission from Elsevier).*

**How to cite:** *Angew. Chem. Int. Ed.* **2015**, *54*, 4160–4181

*Angew. Chem.* **2015**, *127*, 4232–4254

- [1] J. Henderson, J. Evans, K. Nikita, *Mediterr. Archaeol. Archaeometry* **2010**, *10*, 1–24.
- [2] a) B. D. Ratner, A. S. Hoffman, F. J. Schoen, J. S. Lemons, *Biomaterials Science*, Academic Press, San Diego, **1996**; b) L. L. Hench, J. M. Polak, *Science* **2002**, *295*, 1014–1017.
- [3] a) L. L. Hench, R. J. Splinter, W. C. Allen, T. K. Greenlee, *J. Biomed. Mater. Res.* **1971**, *5*, 117–141; b) W. P. Cao, L. L. Hench, *Ceram. Int.* **1996**, *22*, 493–507.
- [4] a) D. L. Wheeler, K. E. Stokes, R. G. Hoellrich, D. L. Chamberland, S. W. McLoughlin, *J. Biomed. Mater. Res.* **1998**, *41*, 527–533; b) S. Froum, S. C. Cho, E. Rosenberg, M. Rohrer, D. Tarnow, *J. Periodontol.* **2002**, *73*, 94–102.
- [5] a) L. L. Hench, *J. Mater. Sci. Mater. Med.* **2006**, *17*, 967–978; b) L. L. Hench, J. W. Hench, D. C. Greenspan, *J. Aust. Ceram. Soc.* **2004**, *40*, 1–42.
- [6] a) A. C. Wright, *The Constitution of Glass*, Society of Glass Technology, Sheffield, **2012**; b) W. E. S. Turner, *J. Soc. Glass Technol. Trans.* **1925**, *9*, 147–166; c) G. Tammann, *J. Soc. Glass Technol. Trans.* **1925**, *9*, 166–185.
- [7] L. L. Hench, D. B. Spilman, J. W. Hench, Patent US 4775646, University of Florida, US, **1988**.
- [8] Ö. H. Andersson, G. Z. Liu, K. H. Karlsson, L. Niemi, J. Miettinen, J. Juhanaja, *J. Mater. Sci. Mater. Med.* **1990**, *1*, 219–227.
- [9] M. Brink, T. Turunen, R. P. Happonen, A. Yli-Urpo, *J. Biomed. Mater. Res.* **1997**, *37*, 114–121.
- [10] J. M. Gomez-Vega, E. Saiz, A. P. Tomsia, T. Oku, K. Suganuma, G. W. Marshall, S. J. Marshall, *Adv. Mater.* **2000**, *12*, 894–898.
- [11] I. Elgayar, A. E. Aliev, A. R. Boccaccini, R. G. Hill, *J. Non-Cryst. Solids* **2005**, *351*, 173–183.
- [12] J. E. Shelby, *Introduction to Glass Science and Technology*, 2nd ed., The Royal Society of Chemistry, Cambridge, **2005**.
- [13] W. H. Zachariasen, *J. Am. Chem. Soc.* **1932**, *54*, 3841–3851.
- [14] L. Lichtenstein, C. Büchner, B. Yang, S. Shaikhutdinov, M. Heyde, M. Sierka, R. Włodarczyk, J. Sauer, H. J. Freund, *Angew. Chem. Int. Ed.* **2012**, *51*, 404–407; *Angew. Chem.* **2012**, *124*, 416–420.
- [15] a) J. R. Jones in *Bio-glasses. An Introduction* (Eds.: J. R. Jones, A. G. Clare), Wiley, New York, **2012**, pp. 29–44; b) J. R. Jones,

- J. Eur. Ceram. Soc.* **2009**, 29, 1275–1281; c) W. Stöber, A. Fink, E. Bohn, *J. Colloid Interface Sci.* **1968**, 26, 62–69.
- [16] a) V. FitzGerald, D. M. Pickup, D. Greenspan, G. Sarkar, J. J. Fitzgerald, K. M. Wetherall, R. M. Moss, J. R. Jones, R. J. Newport, *Adv. Funct. Mater.* **2007**, 17, 3746–3753; b) Y. Xiang, J. C. Du, *Chem. Mater.* **2011**, 23, 2703–2717.
- [17] A. Pedone, G. Malavasi, M. C. Menziani, *J. Phys. Chem. C* **2009**, 113, 15723–15730.
- [18] S. J. Watts, M. D. O'Donnell, R. V. Law, R. G. Hill, *J. Non-Cryst. Solids* **2010**, 356, 517–524.
- [19] A. Pedone, T. Charpentier, G. Malavasi, M. C. Menziani, *Chem. Mater.* **2010**, 22, 5644–5652.
- [20] M. W. G. Lockyer, D. Holland, R. Dupree, *J. Non-Cryst. Solids* **1995**, 188, 207–219.
- [21] D. S. Brauer, N. Karpukhina, R. V. Law, R. G. Hill, *J. Mater. Chem.* **2009**, 19, 5629–5636.
- [22] A. Tilocca, A. N. Cormack, N. H. de Leeuw, *Chem. Mater.* **2007**, 19, 95–103.
- [23] a) R. Hill, *J. Mater. Sci. Lett.* **1996**, 15, 1122–1125; b) R. G. Hill, D. S. Brauer, *J. Non-Cryst. Solids* **2011**, 357, 3884–3887.
- [24] The split network analysis presented by M. Edén and the Stevels parameter  $Y$  described by Strnad use a comparable approach for describing the average network polymerization in oxide glasses: a) M. Edén, *J. Non-Cryst. Solids* **2011**, 357, 1595–1602; b) Z. Strnad, *Biomaterials* **1992**, 13, 317–321.
- [25] M. D. O'Donnell, *Acta Biomater.* **2011**, 7, 2264–2269.
- [26] I. Avramov, R. Keding, C. Rüssel, R. Kranold, *J. Non-Cryst. Solids* **2000**, 278, 13–18.
- [27] a) J. C. Phillips, M. F. Thorpe, *Solid State Commun.* **1985**, 53, 699–702; b) M. F. Thorpe, *J. Non-Cryst. Solids* **1983**, 57, 355–370.
- [28] F. Fayon, C. Duee, T. Poumeyrol, M. Allix, D. Massiot, *J. Phys. Chem. C* **2013**, 117, 2283–2288.
- [29] a) H. Grussaute, L. Montagne, G. Palavit, J. L. Bernard, *J. Non-Cryst. Solids* **2000**, 263, 312–317; b) R. Dupree, D. Holland, M. G. Mortuza, J. A. Collins, M. W. G. Lockyer, *J. Non-Cryst. Solids* **1988**, 106, 403–407.
- [30] A. Tilocca, A. N. Cormack, *J. Phys. Chem. B* **2007**, 111, 14256–14264.
- [31] G. H. Aylward, T. J. V. Findlay, *SI Chemical Data*, 6th ed., Wiley-VCH, Weinheim, **2007**.
- [32] a) R. A. Martin, H. L. Twyman, G. J. Rees, J. M. Smith, E. R. Barney, M. E. Smith, J. V. Hanna, R. J. Newport, *Phys. Chem. Chem. Phys.* **2012**, 14, 12105–12113; b) M. Tylkowski, D. S. Brauer, *J. Non-Cryst. Solids* **2013**, 376, 175–181.
- [33] G. Malavasi, A. Pedone, M. C. Menziani, *J. Phys. Chem. B* **2013**, 117, 4142–4150.
- [34] I. Elgayar, PhD thesis, Imperial College, London, **2004**.
- [35] R. G. Hill, D. S. Brauer, *Acta Biomater.* **2011**, 7, 3601–3605.
- [36] D. S. Brauer, M. N. Anjum, M. Mneimne, R. M. Wilson, H. Doweidar, R. G. Hill, *J. Non-Cryst. Solids* **2012**, 358, 1438–1442.
- [37] D. S. Brauer, R. G. Hill, M. D. O'Donnell, *Phys. Chem. Glasses* **2012**, 53, 27–30.
- [38] G. Lusvardi, G. Malavasi, M. Cortada, L. Menabue, M. C. Menziani, A. Pedone, U. Segre, *J. Phys. Chem. B* **2008**, 112, 12730–12739.
- [39] L. Lefebvre, J. Chevalier, L. Gremillard, R. Zenati, G. Thollet, D. Bernache-Assolant, A. Govin, *Acta Mater.* **2007**, 55, 3305–3313.
- [40] J. Massera, S. Fagerlund, L. Hupa, M. Hupa, *J. Am. Ceram. Soc.* **2012**, 95, 607–613.
- [41] a) A. Dietzel, *Naturwissenschaften* **1941**, 29, 537–547; b) E. M. Rabinovich, *Phys. Chem. Glasses* **1983**, 24, 54–56.
- [42] a) A. Pedone, T. Charpentier, M. C. Menziani, *J. Mater. Chem.* **2012**, 22, 12599–12608; b) D. S. Brauer, A. Al-Noaman, R. G. Hill, H. Doweidar, *Mater. Chem. Phys.* **2011**, 130, 121–125; c) J. K. Christie, A. Pedone, M. C. Menziani, A. Tilocca, *J. Phys. Chem. B* **2011**, 115, 2038–2045.
- [43] A. Dietzel, *Z. Elektrochem.* **1942**, 48, 9–23.
- [44] M. Diba, F. Tapia, A. R. Boccacini, L. A. Strobel, *Int. J. Appl. Glass Sci.* **2012**, 3, 221–253.
- [45] A. Chrissanthopoulos, N. Bouropoulos, S. N. Yannopoulos, *Vib. Spectrosc.* **2008**, 48, 118–125.
- [46] A. Pedone, G. Malavasi, M. C. Menziani, U. Segre, A. N. Cormack, *J. Phys. Chem. C* **2008**, 112, 11034–11041.
- [47] S. Kroeker, J. F. Stebbins, *Am. Mineral.* **2000**, 85, 1459–1464.
- [48] X. Chen, D. S. Brauer, N. Karpukhina, R. D. Waite, M. Barry, I. J. McKay, R. G. Hill, *Mater. Lett.* **2014**, 126, 278–280.
- [49] G. Lusvardi, G. Malavasi, L. Menabue, M. C. Menziani, U. Segre, M. M. Carnasciali, A. Ubaldini, *J. Non-Cryst. Solids* **2004**, 345, 710–714.
- [50] L. Linati, G. Lusvardi, G. Malavasi, L. Menabue, M. C. Menziani, P. Mustarelli, U. Segre, *J. Phys. Chem. B* **2005**, 109, 4989–4998.
- [51] J. M. Smith, R. A. Martin, G. J. Cuello, R. J. Newport, *J. Mater. Chem. B* **2013**, 1, 1296–1303.
- [52] I. Farooq, M. Tylkowski, S. Müller, T. Janicki, D. S. Brauer, R. G. Hill, *Biomed. Mater.* **2013**, 8, 065008.
- [53] a) Y. C. Fredholm, N. Karpukhina, R. V. Law, R. G. Hill, *J. Non-Cryst. Solids* **2010**, 356, 2546–2551; b) K. Fujikura, N. Karpukhina, T. Kasuga, D. S. Brauer, R. G. Hill, R. V. Law, *J. Mater. Chem.* **2012**, 22, 7395–7402; c) R. A. Martin, H. L. Twyman, G. J. Rees, E. R. Barney, R. M. Moss, J. M. Smith, R. G. Hill, G. Cibin, T. Charpentier, M. E. Smith, J. V. Hanna, R. J. Newport, *J. Mater. Chem.* **2012**, 22, 22212–22223.
- [54] H. Morikawa, S. Lee, T. Kasuga, D. S. Brauer, *J. Non-Cryst. Solids* **2013**, 380, 53–59.
- [55] N. H. Ray, *J. Non-Cryst. Solids* **1974**, 15, 423–434.
- [56] Y. C. Fredholm, N. Karpukhina, D. S. Brauer, J. R. Jones, R. V. Law, R. G. Hill, *J. R. Soc. Interface* **2012**, 9, 880–889.
- [57] D. E. Day, *J. Non-Cryst. Solids* **1976**, 21, 343–372.
- [58] M. D. O'Donnell, R. G. Hill, *Acta Biomater.* **2010**, 6, 2382–2385.
- [59] M. D. O'Donnell, S. J. Watts, R. V. Law, R. G. Hill, *J. Non-Cryst. Solids* **2008**, 354, 3554–3560.
- [60] R. Dupree, D. Holland, M. G. Mortuza, *Phys. Chem. Glasses* **1988**, 29, 18–21.
- [61] M. D. O'Donnell, S. J. Watts, R. G. Hill, R. V. Law, *J. Mater. Sci. Mater. Med.* **2009**, 20, 1611–1618.
- [62] G. Lusvardi, G. Malavasi, L. Menabue, V. Aina, C. Morterra, *Acta Biomater.* **2009**, 5, 3548–3562.
- [63] D. S. Brauer, N. Karpukhina, M. D. O'Donnell, R. V. Law, R. G. Hill, *Acta Biomater.* **2010**, 6, 3275–3282.
- [64] M. Bohner, J. Lemaitre, *Biomaterials* **2009**, 30, 2175–2179.
- [65] A. Tilocca, A. N. Cormack, *Langmuir* **2010**, 26, 545–551.
- [66] S. Fagerlund, L. Hupa, M. Hupa, *Acta Biomater.* **2013**, 9, 5400–5410.
- [67] A. Tilocca, A. N. Cormack, *ACS Appl. Mater. Interfaces* **2009**, 1, 1324–1333.
- [68] D. E. Clark, M. F. Dillmore, E. C. Ethridge, L. L. Hench, *J. Am. Ceram. Soc.* **1976**, 59, 62–65.
- [69] A. Tilocca, A. N. Cormack, *Proc. R. Soc. London Ser. A* **2011**, 467, 2102–2111.
- [70] L. L. Hench, D. E. Clark, *J. Non-Cryst. Solids* **1978**, 28, 83–105.
- [71] L. Hupa, K. H. Karlsson, M. Hupa, H. T. Aro, *Glass Technol.* **2010**, 51, 89–92.
- [72] L. L. Hench, *J. Am. Ceram. Soc.* **1991**, 74, 1487–1510.
- [73] I. D. Xynos, M. V. J. Hukkanen, J. J. Batten, L. D. Buttery, L. L. Hench, J. M. Polak, *Calcif. Tissue Int.* **2000**, 67, 321–329.
- [74] S. Fagerlund, P. Ek, L. Hupa, M. Hupa, *J. Am. Ceram. Soc.* **2012**, 95, 3130–3137.
- [75] P. Ducheyne, *J. Biomed. Mater. Res.* **1999**, 46, 301–303.



- [76] K. E. Wallace, R. G. Hill, J. T. Pembroke, C. J. Brown, P. V. Hatton, *J. Mater. Sci. Mater. Med.* **1999**, *10*, 697–701.
- [77] I. Ahmed, P. S. Cronin, E. A. A. Neel, A. J. Parsons, J. C. Knowles, C. D. Rudd, *J. Biomed. Mater. Res. Part B* **2009**, *89B*, 18–27.
- [78] a) X. Chen, X. Chen, D. S. Brauer, R. M. Wilson, R. G. Hill, N. Karpukhina, *Materials* **2014**, *7*, 5470–5487; b) I. Kansal, D. U. Tulyaganov, M. J. Pascual, L. Gremillard, A. Malchere, J. M. F. Ferreira, *J. Non-Cryst. Solids* **2013**, *380*, 17–24.
- [79] R. A. Martin, H. Twyman, D. Qiu, J. C. Knowles, R. J. Newport, *J. Mater. Sci. Mater. Med.* **2009**, *20*, 883–888.
- [80] S. Fujibayashi, M. Neo, H. M. Kim, T. Kokubo, T. Nakamura, *Biomaterials* **2003**, *24*, 1349–1356.
- [81] E. Gentleman, M. M. Stevens, R. G. Hill, D. S. Brauer, *Acta Biomater.* **2013**, *9*, 5771–5779.
- [82] a) J. C. Elliott, *Structure and Chemistry of the Apatites and Other Calcium Orthophosphates*, Elsevier, Amsterdam, **1994**; b) R. Z. LeGeros, O. R. Trautz, E. Klein, J. P. LeGeros, *Experientia* **1969**, *25*, 5–7.
- [83] J. R. Jones, P. Sepulveda, L. L. Hench, *J. Biomed. Mater. Res.* **2001**, *58*, 720–726.
- [84] L. L. Hench, H. A. Paschall, *J. Biomed. Mater. Res.* **1973**, *7*, 25–42.
- [85] T. Kokubo, H. Kushitani, S. Sakka, T. Kitsugi, T. Yamamuro, *J. Biomed. Mater. Res.* **1990**, *24*, 721–734.
- [86] L. Müller, F. A. Müller, *Acta Biomater.* **2006**, *2*, 181–189.
- [87] D. S. Brauer, C. Rüssel, W. Li, S. Habelitz, *J. Biomed. Mater. Res. A* **2006**, *77A*, 213–219.
- [88] a) M. M. Pereira, L. L. Hench, *J. Sol-Gel Sci. Technol.* **1996**, *7*, 59–68; b) P. Saravanapavan, J. R. Jones, R. S. Pryce, L. L. Hench, *J. Biomed. Mater. Res. Part A* **2003**, *66A*, 110–119.
- [89] M. Mneimne, R. G. Hill, A. J. Bushby, D. S. Brauer, *Acta Biomater.* **2011**, *7*, 1827–1834.
- [90] R. J. Newport, L. J. Skipper, D. Carta, D. M. Pickup, F. E. Sowrey, M. E. Smith, P. Saravanapavan, L. L. Hench, *J. Mater. Sci. Mater. Med.* **2006**, *17*, 1003–1010.
- [91] J. J. Videau, V. Dupuis, *Eur. J. Solid State Inorg. Chem.* **1991**, *28*, 303–343.
- [92] X. Lu, Y. Leng, *Biomaterials* **2005**, *26*, 1097–1108.
- [93] R. F. Brown, D. E. Day, T. E. Day, S. Jung, M. N. Rahaman, Q. Fu, *Acta Biomater.* **2008**, *4*, 387–396.
- [94] J. R. Jones, *Acta Biomater.* **2013**, *9*, 4457–4486.
- [95] a) D. S. Brauer, M. Mneimne, R. G. Hill, *J. Non-Cryst. Solids* **2011**, *357*, 3328–3333; b) F. A. Shah, D. S. Brauer, N. Desai, R. G. Hill, K. A. Hing, *Mater. Lett.* **2014**, *119*, 96–99.
- [96] F. A. Shah, D. S. Brauer, R. M. Wilson, R. G. Hill, K. A. Hing, *J. Biomed. Mater. Res. Part A* **2014**, *102*, 647–654.
- [97] a) M. R. Filgueiras, G. La Torre, L. L. Hench, *J. Biomed. Mater. Res.* **1993**, *27*, 445–453; b) M. R. T. Filgueiras, G. La Torre, L. L. Hench, *J. Biomed. Mater. Res.* **1993**, *27*, 1485–1493.
- [98] N. Kanzaki, K. Onuma, G. Treboux, S. Tsutsumi, A. Ito, *J. Phys. Chem. B* **2000**, *104*, 4189–4194.
- [99] J. Massera, L. Hupa, M. Hupa, *J. Non-Cryst. Solids* **2012**, *358*, 2701–2707.
- [100] A. Hoppe, N. S. Güldal, A. R. Boccaccini, *Biomaterials* **2011**, *32*, 2757–2774.
- [101] I. D. Xynos, A. J. Edgar, L. D. K. Buttery, L. L. Hench, J. M. Polak, *Biochem. Biophys. Res. Commun.* **2000**, *276*, 461–465.
- [102] a) E. Gentleman, Y. C. Fredholm, G. Jell, N. Lotfibakhshai, M. D. O'Donnell, R. G. Hill, M. M. Stevens, *Biomaterials* **2010**, *31*, 3244–3252; b) M. D. O'Donnell, P. L. Candarlioglu, C. A. Miller, E. Gentleman, M. M. Stevens, *J. Mater. Chem.* **2010**, *20*, 8934–8941.
- [103] B. Kwakye-Awuah, C. Williams, M. A. Kenward, I. Radecka, *J. Appl. Microbiol.* **2008**, *104*, 1516–1524.
- [104] P. J. Newby, R. El-Gendy, J. Kirkham, X. B. Yang, I. D. Thompson, A. R. Boccaccini, *J. Mater. Sci. Mater. Med.* **2011**, *22*, 557–569.
- [105] J. R. Jones, L. M. Ehrenfried, P. Saravanapavan, L. L. Hench, *J. Mater. Sci. Mater. Med.* **2006**, *17*, 989–996.
- [106] M. Bellantone, N. J. Coleman, L. L. Hench, *Key Eng. Mater.* **2001**, *192*, 597–600.
- [107] G. Lusvardi, G. Malavasi, F. Tarsitano, L. Menabue, M. C. Menziani, A. Pedone, *J. Phys. Chem. B* **2009**, *113*, 10331–10338.
- [108] J. D. B. Featherstone, *J. Am. Dent. Assoc.* **2000**, *131*, 887–899.
- [109] J. Aaseth, M. Shimshi, J. L. Gabilove, G. S. Birketvedt, *J. Trace Elem. Exp. Med.* **2004**, *17*, 83–92.
- [110] a) G. Lusvardi, G. Malavasi, L. Menabue, M. C. Menziani, *J. Phys. Chem. B* **2002**, *106*, 9753–9760; b) G. Lusvardi, D. Zaffe, L. Menabue, C. Bertoldi, G. Malavasi, U. Consolo, *Acta Biomater.* **2009**, *5*, 419–428.
- [111] A. B. G. Lansdown, U. Mirastschijski, N. Stubbs, E. Scanlon, M. S. Agren, *Wound Repair Regen* **2007**, *15*, 2–16.
- [112] a) V. Aina, A. Perardi, L. Bergandi, G. Malavasi, L. Menabue, C. Morterra, D. Ghigo, *Chem.-Biol. Interact.* **2007**, *167*, 207–218; b) D. S. Brauer, E. Gentleman, D. F. Farrar, M. M. Stevens, R. G. Hill, *Biomed. Mater.* **2011**, *6*, 045007.
- [113] V. Aina, G. Malavasi, A. F. Pla, L. Munaron, C. Morterra, *Acta Biomater.* **2009**, *5*, 1211–1222.
- [114] S. J. Watts, PhD thesis, Imperial College, London, **2010**.
- [115] M. M. Azevedo, G. Jell, M. D. O'Donnell, R. V. Law, R. G. Hill, M. M. Stevens, *J. Mater. Chem.* **2010**, *20*, 8854–8864.
- [116] a) A. A. Gorustovich, J. A. Roether, A. R. Boccaccini, *Tissue Eng. Part B* **2010**, *16*, 199–207; b) A. Arkudas, A. Balzer, G. Buehrer, I. Arnold, A. Hoppe, R. Detsch, P. Newby, T. Fey, P. Greil, R. E. Horch, A. R. Boccaccini, U. Kneser, *Tissue Eng. Part C* **2013**, *19*, 479–486.
- [117] A. Hoppe, R. Meszaros, C. Stähli, S. Romeis, J. Schmidt, J. Peukert, B. Marelli, S. N. Nazhat, L. Wondraczek, J. Lao, E. Jallot, A. R. Boccaccini, *J. Mater. Chem. B* **2013**, in press.
- [118] C. Y. Kim, A. E. Clark, L. L. Hench, *J. Non-Cryst. Solids* **1989**, *113*, 195–202.
- [119] K. A. Hing, *Philos. Trans. R. Soc. London Ser. A* **2004**, *362*, 2821–2850.
- [120] a) D. E. Day, J. E. White, R. F. Brown, K. D. McMenamin, *Glass Technol.* **2003**, *44*, 75–81; b) S. B. Jung in *Bio-glasses. An Introduction* (Eds.: J. R. Jones, A. G. Clare), Wiley, New York, **2012**, pp. 75–94.
- [121] E. Vedel, H. Arstila, H. Ylanen, L. Hupa, M. Hupa, *Glass Technol.* **2008**, *49*, 251–259.
- [122] M. D. O'Donnell, S. J. Watts, R. V. Law, R. G. Hill, *J. Non-Cryst. Solids* **2008**, *354*, 3561–3566.
- [123] O. Guillon, S. Y. Cao, J. Y. Chang, L. Wondraczek, A. R. Boccaccini, *J. Eur. Ceram. Soc.* **2011**, *31*, 999–1007.
- [124] H. Arstila, E. Vedel, L. Hupa, M. Hupa, *J. Eur. Ceram. Soc.* **2007**, *27*, 1543–1546.
- [125] H. Arstila, L. Hupa, K. H. Karlsson, M. Hupa, *J. Non-Cryst. Solids* **2008**, *354*, 722–728.
- [126] X. Chatzistavrou, T. Zorba, K. Chrissafis, G. Kaimakamis, E. Kontonasi, P. Koidis, K. M. Paraskevopoulos, *J. Therm. Anal. Calorim.* **2006**, *85*, 253–259.
- [127] The temperature of the onset of crystallization, to be precise.
- [128] P. G. Galliano, J. M. P. Lopez, *J. Mater. Sci. Mater. Med.* **1995**, *6*, 353–359.
- [129] M. Brink, *J. Biomed. Mater. Res.* **1997**, *36*, 109–117.
- [130] H. Arstila, M. Tukiainen, S. Taipale, M. Kellomaki, L. Hupa in *Glass: The Challenge for the 21st Century (Advanced Materials Research Vol. 39–40)* (Eds.: M. Liška, D. Galusek, R. Klement, V. Petrušková), Trans Tech Publications, Stäfa, **2008**, pp. 287–292.

- [131] H. Arstila, E. Vedel, L. Hupa, M. Hupa, *Glass Technol.* **2008**, 49, 260–265.
- [132] A. Mandlule, F. Döhler, L. van Wüllen, T. Kasuga, D. S. Brauer, *J. Non-Cryst. Solids* **2014**, 392–393, 31–38.
- [133] T. Kasuga, Y. Abe, *J. Non-Cryst. Solids* **1999**, 243, 70–74.
- [134] a) O. Peitl, E. D. Zanotto, L. L. Hench, *J. Non-Cryst. Solids* **2001**, 292, 115–126; b) N. Karpukhina, R. G. Hill, R. V. Law, *Chem. Soc. Rev.* **2014**, 43, 2174–2186.
- [135] a) L. L. Hench, *J. Am. Ceram. Soc.* **1998**, 81, 1705–1728; b) W. Vogel, W. Höland, *Angew. Chem. Int. Ed. Engl.* **1987**, 26, 527–544; *Angew. Chem.* **1987**, 99, 541–558.
- [136] J. Chevalier, L. Gremillard, *J. Eur. Ceram. Soc.* **2009**, 29, 1245–1255.
- [137] M. Magallanes-Perdomo, S. Meille, J. M. Chenal, E. Pacard, J. Chevalier, *J. Eur. Ceram. Soc.* **2012**, 32, 2765–2775.
- [138] a) J. Massera, C. Claireaux, T. Lehtonen, J. Tuominen, L. Hupa, M. Hupa, *J. Non-Cryst. Solids* **2011**, 357, 3623–3630; b) S. Fagerlund, J. Massera, M. Hupa, L. Hupa, *J. Eur. Ceram. Soc.* **2012**, 32, 2731–2738.
- [139] M. N. Rahaman, D. E. Day, B. S. Bal, Q. Fu, S. B. Jung, L. F. Bonewald, A. P. Tomsia, *Acta Biomater.* **2011**, 7, 2355–2373.
- [140] D. Groh, F. Döhler, D. S. Brauer, *Acta Biomater.* **2014**, 10, 4465–4473.
- [141] Z. Y. Wu, R. G. Hill, S. Yue, D. Nightingale, P. D. Lee, J. R. Jones, *Acta Biomater.* **2011**, 7, 1807–1816.
- [142] a) N. Lotfikhshah, D. S. Brauer, R. G. Hill, *J. Non-Cryst. Solids* **2010**, 356, 2583–2590; b) D. S. Brauer, R. M. Wilson, T. Kasuga, *J. Non-Cryst. Solids* **2012**, 358, 1720–1723.
- [143] Q. Z. Z. Chen, I. D. Thompson, A. R. Boccacini, *Biomaterials* **2006**, 27, 2414–2425.
- [144] a) D. S. Brauer, C. Rüssel, S. Vogt, J. Weisser, M. Schnabelrauch, *J. Biomed. Mater. Res. A* **2007**, 80A, 410–420; b) W. Liang, C. Rüssel, *J. Mater. Sci.* **2006**, 41, 3787–3792.
- [145] L. Wondraczek, J. C. Mauro, J. Eckert, U. Kuehn, J. Horbach, J. Deubener, T. Rouxel, *Adv. Mater.* **2011**, 23, 4578–4586.
- [146] a) X. Liu, M. N. Rahaman, Q. A. Fu, *Acta Biomater.* **2011**, 7, 406–416; b) X. Liu, M. N. Rahaman, Q. Fu, A. P. Tomsia, *Acta Biomater.* **2012**, 8, 415–423.
- [147] X. Liu, M. N. Rahaman, G. E. Hilmas, B. S. Bal, *Acta Biomater.* **2013**, 9, 7025–7034.
- [148] a) Q. Fu, E. Saiz, M. N. Rahaman, A. P. Tomsia, *Mater. Sci. Eng. C* **2011**, 31, 1245–1256; b) Q. Fu, E. Saiz, M. N. Rahaman, A. P. Tomsia, *Adv. Funct. Mater.* **2013**, 23, 5461–5476.
- [149] J. R. Jones, R. C. Atwood, G. Poologundarampillai, S. Yue, P. D. Lee, *J. Mater. Sci. Mater. Med.* **2009**, 20, 463–471.
- [150] E. S. Place, N. D. Evans, M. M. Stevens, *Nat. Mater.* **2009**, 8, 457–470.
- [151] a) D. Wang, G. Poologundarampillai, W. van den Bergh, R. J. Chater, T. Kasuga, J. R. Jones, D. S. McPhail, *Biomed. Mater.* **2014**, 9, 015013; b) G. Poologundarampillai, D. Wang, S. Li, J. Nakamura, R. Bradley, P. D. Lee, M. M. Stevens, D. S. McPhail, T. Kasuga, J. R. Jones, *Acta Biomater.* **2014**, 10, 3733–3746.
- [152] X. Liu, M. N. Rahaman, D. E. Day, *J. Mater. Sci. Mater. Med.* **2013**, 24, 583–595.
- [153] M. Marcolongo, P. Ducheyne, J. Garino, E. Schepers, *J. Biomed. Mater. Res.* **1998**, 39, 161–170.
- [154] Y. Yue, C. Rüssel, G. Carl, M. Braun, C. Jäger, *Phys. Chem. Glasses* **2000**, 41, 12–16.
- [155] M. Braun, Y. Yue, C. Rüssel, C. Jäger, *J. Non-Cryst. Solids* **1998**, 241, 204–207.
- [156] a) D. C. Clupper, J. E. Gough, P. M. Embanga, I. Nottingher, L. L. Hench, M. M. Hall, *J. Mater. Sci. Mater. Med.* **2004**, 15, 803–808; b) E. Pirhonen, L. Moimas, M. Brink, *Acta Biomater.* **2006**, 2, 103–107.
- [157] F. Quintero, J. Pou, R. Comesaña, F. Lusquinos, A. Riveiro, A. B. Mann, R. G. Hill, Z. Y. Wu, J. R. Jones, *Adv. Funct. Mater.* **2009**, 19, 3084–3090.
- [158] E. Pirhonen, H. Niiranen, T. Niemela, M. Brink, P. Tormala, *J. Biomed. Mater. Res. B* **2006**, 77B, 227–233.
- [159] Y. C. Tsui, C. Doyle, T. W. Clyne, *Biomaterials* **1998**, 19, 2015–2029.
- [160] L. L. Hench, P. J. Buscemi, Patent US 4234972, University of Florida, US, **1980**.
- [161] W. R. Lacefield, L. L. Hench, *Biomaterials* **1986**, 7, 104–108.
- [162] D. Bellucci, V. Cannillo, A. Sola, *Ceram. Int.* **2011**, 37, 2963–2972.
- [163] a) S. Foppiano, S. J. Marshall, G. W. Marshall, E. Saiz, A. P. Tomsia, *Acta Biomater.* **2007**, 3, 765–771; b) Ö. H. Andersson, K. H. Karlsson, H. Hero, E. Vedel, A. Yli-Urpo, K. J. J. Pajamäki, T. S. Lindholm, *J. Mater. Sci. Mater. Med.* **1995**, 6, 242–247.
- [164] S. Foppiano, S. J. Marshall, E. Saiz, A. P. Tomsia, G. W. Marshall, *Acta Biomater.* **2006**, 2, 133–142.
- [165] S. Foppiano, S. J. Marshall, G. W. Marshall, E. Saiz, A. P. Tomsia, *J. Biomed. Mater. Res. A* **2004**, 71A, 242–249.
- [166] R. Müller, *J. Therm. Anal.* **1989**, 35, 823–835.
- [167] T. J. Webster, C. Ergun, R. H. Doremus, R. W. Siegel, R. Bizios, *J. Biomed. Mater. Res.* **2000**, 51, 475–483.
- [168] G. C. Reilly, S. Radin, A. T. Chen, P. Ducheyne, *Biomaterials* **2007**, 28, 4091–4097.
- [169] a) L. Bergandi, V. Aina, S. Garetto, G. Malavasi, E. Aldieri, E. Laurenti, L. Matera, C. Morterra, D. Ghigo, *Chem.-Biol. Interact.* **2010**, 183, 405–415; b) L. Bergandi, V. Aina, G. Malavasi, C. Morterra, D. Ghigo, *Chem.-Biol. Interact.* **2011**, 190, 179–186.
- [170] M. Gubler, T. J. Brunner, M. Zehnder, T. Waltimo, B. Sener, W. J. Stark, *Int. Endodontic J.* **2008**, 41, 670–678.
- [171] a) E. Munukka, O. Leppäranta, M. Korkeamäki, M. Vaahtio, T. Peltola, D. Zhang, L. Hupa, H. Ylänen, J. I. Salonen, M. K. Viljanen, E. Eerola, *J. Mater. Sci. Mater. Med.* **2008**, 19, 27–32; b) D. Zhang, O. Leppäranta, E. Munukka, H. Ylänen, M. K. Viljanen, E. Eerola, M. Hupa, L. Hupa, *J. Biomed. Mater. Res. A* **2010**, 93A, 475–483.
- [172] H. Oonishi, L. L. Hench, J. Wilson, F. Sugihara, E. Tsuji, M. Matsuura, S. Kin, T. Yamamoto, S. Mizokawa, *J. Biomed. Mater. Res.* **2000**, 51, 37–46.
- [173] H. Oonishi, L. L. Hench, J. Wilson, F. Sugihara, E. Tsuji, S. Kushitani, H. Iwaki, *J. Biomed. Mater. Res.* **1999**, 44, 31–43.
- [174] E. J. G. Schepers, P. Ducheyne, *J. Oral Rehabil.* **1997**, 24, 171–181.
- [175] The network connectivities or Stevels parameters in the original publication by Strnad<sup>[26]</sup> were calculated assuming presence of Si-O-P bonds in the glass and are thus too low.
- [176] K. R. Rust, G. T. Singleton, J. Wilson, P. J. Antonelli, *Am. J. Otol.* **1996**, 17, 371–374.
- [177] I. Kinnunen, K. Aitasalo, M. Pollonen, M. Varpula, *J. Cranio Maxillofac. Surgery* **2000**, 28, 229–234.
- [178] H. R. Stanley, M. B. Hall, A. E. Clark, C. J. King, L. L. Hench, J. J. Berte, *Int. J. Oral Maxillofac. Implants* **1997**, 12, 95–105.
- [179] A. M. Gatti, G. Valdrè, O. H. Andersson, *Biomaterials* **1994**, 15, 208–212.
- [180] N. C. Lindfors, *Bone* **2009**, 45, 398–400.
- [181] N. C. Lindfors, I. Koski, J. T. Heikkilä, K. Mattila, A. J. Aho, *J. Biomed. Mater. Res. B* **2010**, 94B, 157–164.
- [182] N. C. Lindfors, *J. Biotechnol. Biomater.* **2011**, 1, 1000111.
- [183] N. C. Lindfors, J. T. Heikkilä, A. J. Aho, *J. Biomed. Mater. Res. B* **2008**, 87B, 73–76.
- [184] R. Hill, S. Rawlinson, G. Davis, S. Nehete, S. Shahdad, *Eur. Cells Mater.* **2014**, 28, 51.
- [185] J. D. B. Featherstone, *Adv. Dent. Res.* **2009**, 21, 4–7.
- [186] A. K. Burwell, L. J. Litkowski, D. C. Greenspan, *Adv. Dent. Res.* **2009**, 21, 35–39.
- [187] R. H. Dababneh, A. T. Khouri, M. Addy, *Br. Dent. J.* **1999**, 187, 606–611.

- [188] a) A. P. Forsback, S. Areva, J. I. Salonen, *Acta Odontol. Scand.* **2004**, 62, 14–20; b) M. Vollenweider, T. J. Brunner, S. Knecht, R. N. Grass, M. Zehnder, T. Imfeld, W. J. Stark, *Acta Biomater.* **2007**, 3, 936–943.
- [189] A. Banerjee, M. Hajatdoost-Sani, S. Farrell, I. Thompson, *J. Dent.* **2010**, 38, 475–479.
- [190] E. Lynch, D. S. Brauer, N. Karpukhina, D. G. Gillam, R. G. Hill, *Dent. Mater.* **2012**, 28, 168–178.
- [191] X. Chen, R. Hill, N. Karpukhina, *Int. J. Appl. Glass Sci.* **2014**, 5, 207–216.

Received: May 15, 2014

Revised: October 20, 2014

Published online: March 12, 2015

# REPRINTS & POSTERS

To do

Order Now!

E-MAIL:

CHEM-REPRINTS@WILEY.COM

WILEY-VCH

- Reprints of your article
- High resolution PDF
- Personalized reprints and PDF
- Posters – available of all the published covers in A1 or A2